POLITECNICO
DI TORINO

FCA

FIAT CHRYSLER AUTOMOBILES

Evaluation of the Potential of Low - Voltage Electrification Technologies for CO_2 Reduction

Master of Science in Mechanical Engineering

Department of Mechanical and Aerospace Engineering

Supervisors:

Prof. Ezio Spessa

Prof.ssa Daniela Anna Misul

Dott. Carloandrea Malvicino

Ing. Maria Rita Solinas

Candidate:

Corrado Maria Milan

Turin, April 2018

Abstract

The increasing number of vehicles produced and sold, especially in developing countries, resulted in grown levels of pollutants in the air, which affect global warming and humans' health. Eco-friendly transportation has therefore become a key issue in today's society, as the strong dependence on fossil fuels of the transportation sector is no longer sustainable. Worldwide CO_2 emission targets will be progressively tightened and a new type approval procedure is currently under implementation, aimed at better reflecting real driving condition. In this context hybrid powertrains, and particularly micro and mild configurations, seem to be the most promising and viable path to respect the limits in the near future.

The purpose of this thesis is to investigate the potential of low voltage electrification technologies for CO_2 emissions reduction in passenger cars. A brief description of the European regulatory framework in the field of CO_2 is presented, followed by an overview on hybrid architectures and a focus on low voltage solutions. The analysis of the case study, represented by an A-segment car equipped with a 12V Belt Starter Generator, has been carried out by means of a mathematical model developed in Matlab/Simulink ambient. In this layout, the conventional alternator is replaced by a more powerful electric machine, which allows the introduction of fuel-saving functionalities such as Advanced Stop&Start, Regenerative Braking and Torque Assist. The benefits in terms of fuel consumption and CO_2 emissions over a baseline version have been quantified on the NEDC and WLTP homologation cycles, performing a sensitivity analysis on the components sizing afterwards. The results have then been employed to perform a cost-benefit evaluation from both the manufacturer and customer perspectives.

Acknowledgments

First of all I would like to express my sincere gratitude to Dott. Carloandrea Malvicino, for giving me the opportunity to work at FCA on this thesis and for the valuable and enlightening advices. I also wish to thank his collaborator, Ing. Maria Rita Solinas, for her kindness and availability.

I am indeed grateful to Prof. Ezio Spessa and Prof.ssa. Daniela Anna Misul, for providing a fundamental contribution to the fulfilment of this project.

Finally, a special thank goes to my family, and particularly to my mom, for the unconditional love and support that I have been given throughout the course of the studies.

Summary

List of Figures

List of Tables

1 Introduction

Over the last decades, we have experienced a worldwide permanent growth in demand of passenger cars, despite the incessant technological progress in the transportation sector has led to the introduction of various alternatives for individual mobility. To many the automobile still remains the most convenient solution for the daily commute, and sometimes it is the only way to fulfil the need to move rapidly and randomly. Moreover, the analysis carried out by ACEA (Figure 1.1) highlights that developing countries, such as China, are driving the trend; thanks to the rising standard of living, a greater share of the population has now the financial resources for a personal means of transportation.

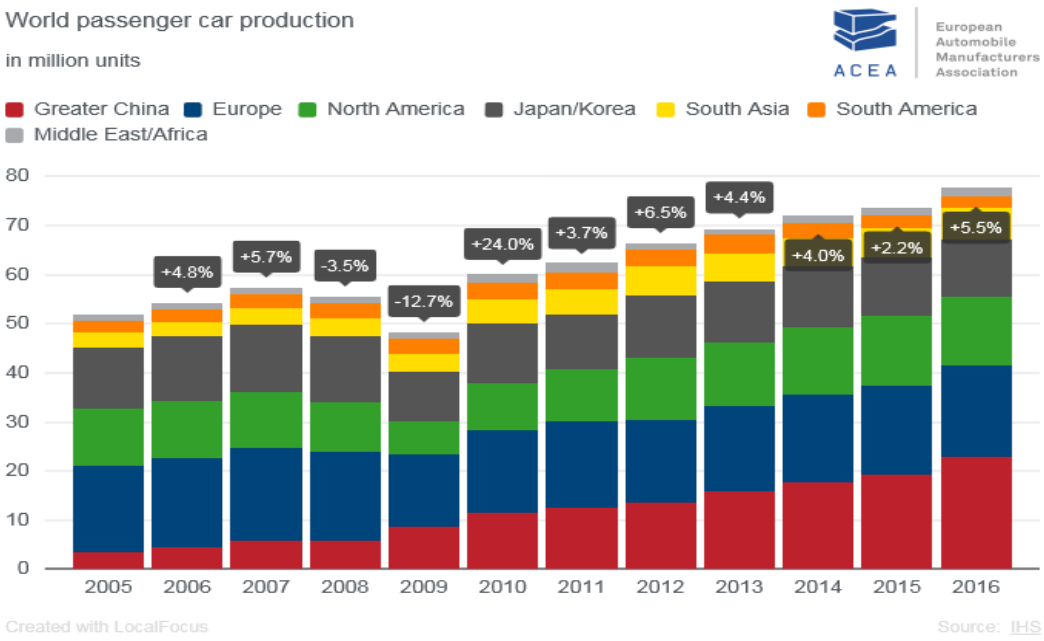

Figure 1.1: World passenger car production trend [1]

For the near future further increases in production volumes are expected, and the greater number of vehicles pouring into the roads is driving the development of alternative high-efficiency technologies. The reason being is

that the transportation sector is based on oil and liquid fuels in general as the primary energy source: considering that the combustion process originates CO_2 as a direct product [2], this dependence explains why this branch plays a key role in greenhouse gases (GHG) emissions:

$$C_xH_y + \left(x + \frac{y}{4}\right)(O_2 + 3.773N_2) = xCO_2 + \frac{y}{2}H_2O + 3.773(x + \frac{y}{4})N_2$$

Among greenhouse gases, i.e. Methane CH_4, Nitrous Oxide N_2O, Ozone O_3 or Water Vapour, CO_2 is not regarded as the most dangerous, but considering the strong impact on global warming it is a topic that has gained more and more importance over the years. The GHG in fact regulate the equilibrium between incoming and reflected energy: most of the solar radiation is absorbed by the Earth's surface and warms it, while the remaining part is reflected. Some of the reflected heat is then trapped and re-emitted by greenhouse gases, warming up the lower atmosphere and leading to global temperature increase and climate instability [2]. To make matters worse, oil combustion has another drawback: the burning process in internal combustion engines (ICE) originates in fact a series of primary and secondary pollutants that deteriorate air quality and represent a threat to human health.

A study published by the International Energy Agency reveals that the transportation sector is responsible for almost 24% of the CO_2 emitted worldwide [3], and a relevant percentage is related to private and commercial road transportation.

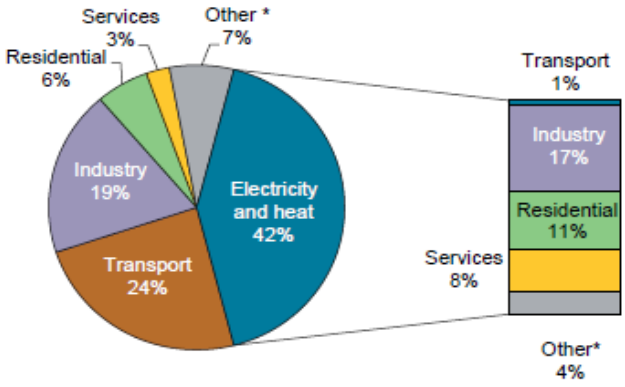

Figure 1.2: Worldwide CO2 emissions by sector, 2015 [3]

Considering the other means of transportation, a substantial contribution is coming from marine bunkers and air travel, with the latter that has more than doubled its emissions over the period 1990-2015.

Analyzing the data in Figure 1.2, it must be pointed out that they underestimate the real impact on global CO_2 level by focusing only on the vehicle direct emissions (*Tank-to-Wheel* approach), whereas a more detailed approach should also take into account the emissions related to the whole manufacturing process (*Well-to-Wheel* approach), worsening the depicted scenario.

In addition to the above-mentioned issues concerning fossil fuels usage, oil reserves on Earth are limited and therefore destined to end. Over the past decades, the evaluation of the status of the reserves has been an intricate matter, source of debates and discussions with sometimes misleading results. Oil sources can be gathered into two groups: *conventional sources*, including crude oil, natural gas liquids, condensate liquids, and *non-conventional sources*, including oil sands, extra heavy oil and oil shade. The former category refers to the oil that can be extracted from the ground via traditional drilling methods, liquid at atmospheric temperature and pressure conditions. It is opposed to unconventional oil, which requires advanced, more expensive and complex extraction methods due to its properties [4].

Currently, conventional sources account for a large part of the oil produced worldwide, but several reservoirs have already been exploited limiting the availability for future extraction. An increase in demand is expected by 2030, 103.8 md/b compared to 82.3 md/b in 2007 [5], with a consistent share attributable to the transportation sector.

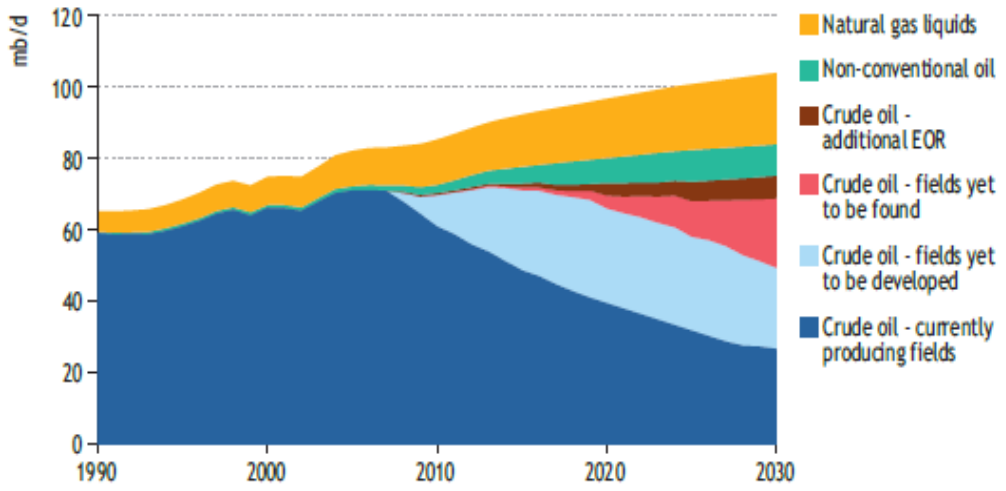

Figure 1.3: World oil production by source [5]

The Reference Scenario presented in the 2008 World Energy Outlook (Figure 1.3) shows that crude oil from currently producing deposits will fulfil less than 40% of the global request by 2030, meaning that the remanence will have to come from oilfields that are not yet operative. Consequently, even though there are large amounts of sources left, the costs for exploiting the residual volume of oil are inevitably destined to raise. The market is going to be constrained by the lack of oil availability, meaning that the current model of individual mobility is inevitably destined to change over the next decades, and cars manufactures will have to put a greater deal of effort into the research of sustainable alternatives to oil.

2 European CO_2 Legislation Framework

This chapter provides an overview of the European legislation framework regarding CO_2, from the origins up to the previsions for the near future. The impact of the new testing procedure, introduced in September 2017, is analysed as well.

2.1 History of the Regulation

The air quality deterioration has been a topic of growing interest since the late sixties, when the economic boom was accompanied by a sudden increase in vehicle sales and, consequently, by a rising concentration of pollutants in metropolitan areas.

With respect to carbon dioxide emissions, the very first targets for passenger cars were set in the late nineties, on the basis of a voluntary agreement between the European Commission and three manufacturer associations: ACEA, JAMA and KAMA. The limit corresponded to a fleet average CO_2 emission of 140 g/km by 2008 for passenger cars, but in 2004 it was clear that manufacturers could not keep their word: in response, mandatory targets were imposed by the Commission. Since then, annual CO_2 reduction rates for cars augmented from 1 percent to about 4 percent [2].

2.2 Emission Targets

The targets imposed by the European Commission have to be met by manufacturers following a precise Type Approval procedure, in order to be allowed to introduce a new vehicle model on the market. The New European Driving Cycle (NEDC) is the prescribed driving cycle for the determination of fuel consumption and pollutant emissions in Europe: it is performed on a chassis dynamometer and its standardization was intended to guarantee repeatability and comparability of the results.

2.2.1 2008 Targets

In December 2008, the European Union imposed to all manufacturers a fleet average target of 130 g/km by the beginning of 2012. The objective for 2020 was fixed at 95 g/km, and it was agreed to complete the regulatory framework with further measures, aimed at achieving a supplementary reduction of 10 g/km. Small manufacturers, producing less than ten thousand units per year, were allowed to have a higher CO_2 emission value, depending on the average weight of their vehicle fleet. For light-commercial vehicles (LCV) a similar approach was used, with the regulation introduced in 2011 that set a limit of 175 g/km fully phased-in by 2016 [2,6].

2.2.2 2015 Targets

To allow manufacturers some time to adapt their fleet to the new targets, the 130 g/km limit was gradually phased-in over the period 2012 - 2015, and adapted basing on the vehicle mass. The final compromise required manufacturers to meet the fleet average target by 65% in 2012, 75% in 2013, 80% in 2014 and 100% from 2015. The target is represented by the *Specific Emission of CO_2* (g/km) of each new passenger car registered in that calendar year:

$$\textit{Specific Emission of } CO_2 = 130 + 0.0457*(M-M_o) \text{ [g/km]}$$

where M is the mass of the vehicle in kg and M_o is 1372 kg for calendar years 2012-2015. The regulation also confirms the long-term target of 95 g/km to be reached by the end of 2020.

Significant results have been achieved: from 2006, within six years the average amount of CO_2 emitted from a new car decreased from about 160 g/km to 132 g/km, a 17% reduction with respect to the European driving cycle NEDC. Moreover, the annual reduction rate has doubled its value compared to the period preceding the introduction of mandatory emission targets [2, 6].

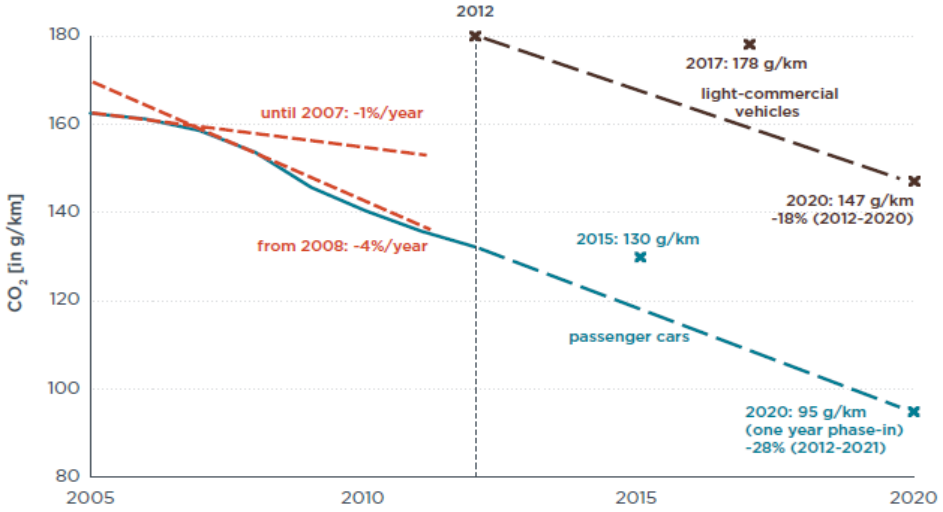

Figure 2.1: Historical development and future targets for CO2 emissions levels [6]

2.2.3 2020 Targets

In April 2013, The Environment Committee of the European Parliament adopted a proposal that confirms the CO_2 target of 95 g/km by 2020 for passenger cars (147 g/km for LCV). This corresponds to a fuel economy of about 3.8 litres per 100 kilometres and to a 27 percent reduction compared to 2015 on a NEDC basis.

Several key-elements of the regulation must be taken into consideration to understand how manufacturers are going to respect the upcoming constraints [6]:

- The fleet average target of 95 g/km of CO_2 requires 95 percent of the new vehicles sold to respect the limit in 2020, and 100 percent from the end of 2020 onwards. Effectively, the target applies therefore from 2021 on;
- Vehicle mass is still considered the most influencing factor for fuel consumption, so the heavier the manufacturer's car fleet, the higher the CO_2 limit allowed. The selected correction factor is 0.0333, which

corresponds to a bonus of 3,33 g/km of CO_2 allowed for every additional 100 kg of vehicle weight;

- As in previous regulations, low-emitting vehicles benefit from *super-credits.* Over the period 2020 - 2022, different weighting factors will be used to consider every car with CO_2 emissions of less than 50 g/km (2.00 to 1.33). The maximum benefit recognised for the use of these credits is equal to 7.5 g/km, compared to the average fleet emission obtained without the application of this measure;
- Introduction of a new test procedure from September 2017, the *Worldwide Harmonized Light Vehicles Test Procedure* (WLTP): without a doubt it is the most substantial modification, aimed at finding a solution to the inadequacy of the *New European Driving Cycle* (NEDC). This aspect is analysed more accurately in Section 2.3.
  The current targets will be adapted to the newly introduced regulation by means of the ongoing correlation studies, to ensure the same standard of severity for every manufacturer and class of vehicles;
- *Eco-innovations* : these technologies, such as e-clutch, high efficiency lights or eco driving and navigation, reduce CO_2 emission in real life, but this benefit is not adequately evaluated by the homologation cycle. To promote their diffusion, manufacturers can apply for a maximum discount of 7 g/km at fleet level;
- Excess emission premiums are provided for those failing to comply with their mandatory emission targets: €95 per vehicle for each gram of exceedance from 2019 onwards;
- To further reduce the divergence between real-world and approval-test emissions, new requirements known as *Real Driving Emissions* (RDE) are being introduced. The RDE is performed during vehicle operation on the road using a portable emissions monitoring system (PEMS). The test will be implemented in September 2017 for new

types of cars and will apply for all registrations from September 2019;

In addition to the above-mentioned measures, a review clause to establish CO_2 emission targets for the period beyond 2020 is present, to ensure that the trajectory delineated for the emissions reduction is maintained. The indicative target stated by the European Parliament range for 2025 is 68-78 g/km [6].

Within the spring of 2018, the European Commission is also likely to propose mandatory standards for the emissions coming from heavy-duty vehicles, as Europe is the only major market in the world that still has not envisaged any regulation in this field.

2.2.4 Post 2020 scenario

The European Union has agreed on the imposition of a target for the reduction of GHG emissions by 40% for 2030, if compared to 1990 levels. For those sectors, such as transportation, that are not involved in the EU's emissions trading scheme, the overall average reduction in annual GHG emissions required by 2030 is 30% below 2005 levels. It is likely that the transportation sector will have to overachieve this target, considering the modest contribution that will come from sectors like agriculture or building, estimated in less than 30%. As a result, over the period 2021 - 2030 passenger cars and light duty vehicles are expected to lower the emissions by 9% annually, which corresponds to an overall 58% drop for the average new vehicle [7].

In terms of current type approval procedure (NEDC), the expected target for passenger cars in 2030 is roughly 40 g/km, and in the hypothesis that a constant trend of reduction is maintained the intermediate target for 2025 is 65 g/km. Concerning WLTP, the definition of future standards is more complex as the regulatory framework is not well-defined yet. In Section 2.3.2

two possible scenarios are presented, with respect to the use of different approaches for the *correlation factors*.

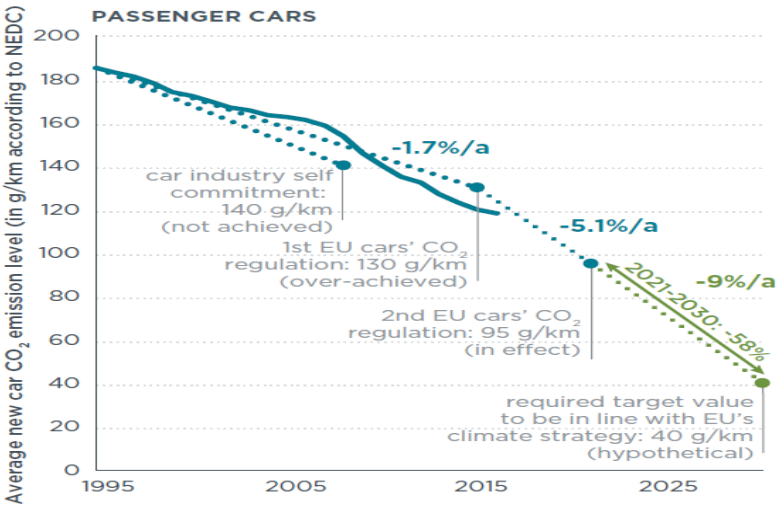

Figure 2.2: Historical development and future scenario for CO2 targets [7]

2.2.5 Extra-EU CO_2 targets

Differing approaches to emission targets are adopted across the world, pursuing the global challenge for CO_2 reduction.

The United States are currently adopting the FTP 75 emission test, with more stringent limits for 2020 and any intention to adopt the WLTP. There are two sets of parallel standards, the *Corporate average fuel economy* (CAFE) and the Greenhouse Gas Emission standards adopted by the *US Environmental Protection Agency* (EPA). The former requires each manufacturer to meet a target, assigned according to vehicle "footprint", for the sales-weighted fuel economy for the entire fleet [2].

China and Japan are about to switch from NEDC and JC 08 test procedures to WLTP, lowering the emission targets to values considerably higher than the European equivalents. However, US and Japan governments are providing consistent financial support and China is increasing taxes to achieve top down targets for an increase in electric vehicles. The following Figure summarizes the in-force and future CO_2 emissions targets worldwide.

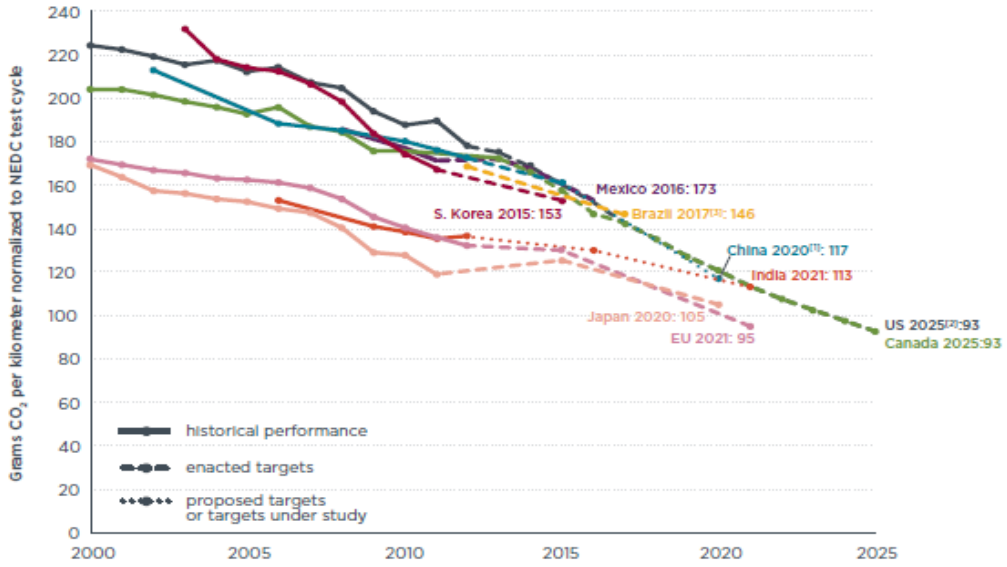

Figure 2.3: Global CO2 targets [g/km] for passenger cars, NEDC [6]

2.3 Transition from NEDC to WTLP

The NEDC is gradually going to be replaced by the WLTP, and the newly developed procedure will differ from the current one and impact on the determination of emission values in Europe. Until now vehicles homologation procedures have been conducted in a laboratory environment, where it is easier to monitor factors which have a heavy influence on the amount of pollutant produced, making the application of test-oriented improvements relatively easy. Consequently, the values obtained from official laboratory tests turned out to be substantially different from the fuel consumptions experienced by the customers in real-world driving conditions, and the discrepancy has been quantified in 15% higher CO_2 emissions on average [8]. In this regard, the European Union commonly agreed to revise the current type approval procedure, in order to reduce the divergence and evaluate more accurately the actual impact of CO_2 reduction technologies.

The NEDC mild accelerations and decelerations, along with the frequent stops, have been proven not to reflect the modern driving manners, and the procedure allows for modifications of the vehicle that do not occur in real conditions and heavily affect CO_2 emissions, such as the use of worn-out tyres with unusually high pressures to reduce the rolling resistance or the elimination of any optional equipment to lower the kerb mass. Moreover, the current regulation provides tolerances on the speed profile of the driving cycle, on temperatures and measuring devices, that, although meant to limit unwanted deviations, result in variations from the expected target values. These tolerance bands are likely to be restricted or eliminated with the upcoming test protocol, thanks to the use of improved testing equipment and methodologies [9].

2.3.1 The new Driving Cycle

The changes introduced by the new certification test are significant, mainly related to the structure of the test-cycle and to the restrictions in terms of starting temperature and vehicle mass. Experts are therefore investigating the topic to derive a NEDC to WLTP conversion factor, that estimates the impact of the transition on CO_2 emission levels.

Table 2.1 reports the representative parameters of both driving cycles.

	NEDC	**WLTP**	**Units**
Start condition	cold	cold	
Duration	1180	1800	s
Distance	11,03	23,27	km
Max Speed	120,0	131,3	km/h
Average Speed	33,6	46,5	km/h
Max Acceleration	1,04	1,67	m/s^2
Mean Acceleration	0,59	0,41	m/s^2
Min Deceleration	-1,39	-1,50	m/s^2
Mean Deceleration	-0,82	-0,45	m/s^2

Durations			
Stop	280	226	s
Constant Speed	475	66	s
Acceleration	247	789	s
Deceleration	178	719	s
Shares			
Stop	23,7%	12,6%	
Constant Speed	40,3%	3,7%	
Acceleration	20,9%	43,8%	
Deceleration	15,1%	39,9%	

Table 2.1: Homologation cycles characteristics [9]

The NEDC is composed of two parts, introduced in 1970 and 1990 respectively and intended to simulate real driving condition in both urban and extra-urban driving conditions. The urban driving part (UDC) consists in the repetition of four ECE-15 cycles, each with a maximum speed of 50 km/h and a duration of 195 seconds. The following extra-urban driving part (EUDC) lasts 400 seconds, with a top speed of 120 km/h and a covered distance of 6.95 kilometres [10].

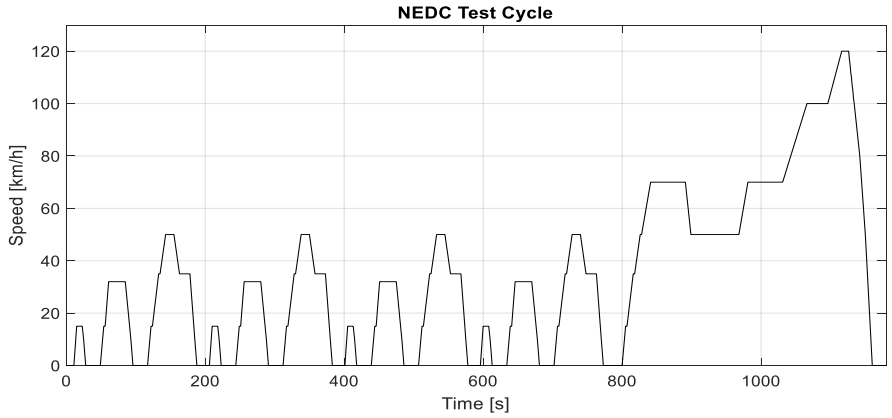

Figure 2.4: NEDC test cycle speed profile

The WLTP is made up of different driving cycles, applicable to a vehicle with respect to the power-to-mass ratio (PMR) and maximum speed.

Class	Phases	PMR [W/kg]
1	Low	< 22
2	Low, Medium, High	22<PMR<34
3	Low, Medium, High, Extra-high	> 34

Table 2.2: WLTP test cycle phases

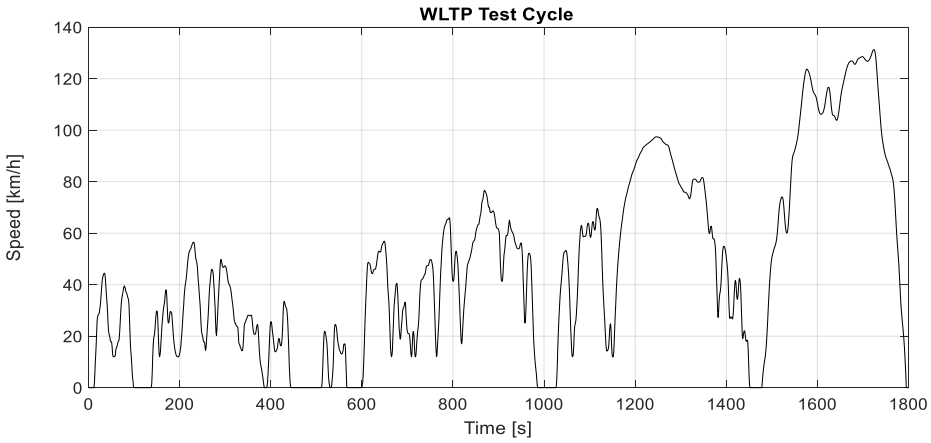

Figure 2.5: WLTP test cycle speed profile

Comparing the two homologation cycles, the following differences can be observed [9]:

- *Cold Start:* considering the longer duration of the newly introduced test cycle, the contribution to the total emission of the cold start for WLTC is about half of the NEDC contribution. During the early stages of driving, the CO_2 emissions increase due to the higher mechanical frictions;
- *Engine load:* Being the WLTC more dynamic than the NEDC, it imposes higher speeds and stronger accelerations, which result in in an increase of the engine loads. On the other hand, internal combustion engines usually perform better at higher engine load, as a consequence of the reduced losses from friction and gas flow. This is reason behind the relatively low efficiency of present engine technologies under the light load typical of NEDC. For these operating

conditions, the expected improvements in engine efficiency are greater than those expected for high loads, thus making the WLTC more demanding in this respect;

- *Engine speed:* this aspect has a direct impact on carbon dioxide emissions. If the engine is spinning faster, the CO_2 performance is worse because of the increased frictions and pumping losses; for this reason, automatic transmissions control logics are designed specifically to achieve low rpms. In the NEDC, a prearranged path for gear shift points is imposed for vehicles equipped with a manual gearbox , whereas for the WLTC they will be adapted to the individual peculiarities of the tested car. As in the WLTC shifting points occur at lower engine speeds compared to the NEDC, this method will result in lower CO_2 emission for manual transmission vehicles;

- *Stop time:* For the WLTC, the stop share is reduced compared to the NEDC (12,6% vs 23,7%), therefore the CO_2 savings related to the *Start&Stop* technology will be lower than in the NEDC.

In contrast to the NEDC procedure, the actual test-mass will be determined for each variant of the same family, considering both optional equipment and vehicle payload to explore every possible combination. However, the versions effectively tested will only be two: one corresponding to the least energy demanding configuration and the other to the highest one, with all the optional equipment on board. The emission values of all the other variants will be obtained by interpolation. Furthermore, the WLTP requires adding 100 kg plus 15% of the maximum vehicle load allowed, resulting in an overall increase of the mass of 8.8% compared to the NEDC. Considering that a 10% mass change corresponds to a 4% CO_2 emission variation, the impact on fuel consumption and CO_2 emission is approximately 3.5% [9]. Lastly, more stringent requirements are introduced for engine start temperature, set at 23 ± 5 °C in the new procedure, and the EU is planning to a adopt a test

temperature much more representative of the average European conditions, 14 °C. Compared to the NEDC range (20 to 30 °C), the lowering will result in higher CO_2 emissions levels.

2.3.2 Correlation Factors and Future WLTP Targets

The approach towards air pollutants in general and CO_2 emissions will be slightly different: the limitations will remain identical under WLTP conditions for the first ones, whereas for the CO_2 targets it was decided to use a dedicated software, *CO_2MPAS,* for the determination of specific NEDC-WLTP correlation factors*.* The WLTP has been introduced to find a solution to the inadequacies of the NEDC, that allowed car makers to declare lower CO_2 values, and taking all these aspects into account the average correlation factor is expected to be around 1,15. For this reason, the CO_2 emissions measured by means of the new type approval procedure will be about 15% higher with respect to the correspondent NEDC values simulated by CO_2MPAS. The correlation factor is likely to increase to 1,25 by 2020, as a consequence of the increased efficiency of the new fleets [7] .

The 2021 WLTP limit can therefore be calculated by multiplying the 2020 NEDC target by the specific fleet average correlation factor. Assuming that all the manufacturers are able to respect their 2020 limits, the 95 g/km NEDC target would correspond to 119 g/km for the WLTP. This would be the basis for any post-2021 revision, and considering an average 20% CO_2 reduction between 2021 and 2030 the resulting target would be about 108 g/km for 2025, and 95 g/km for 2030. In a worst-case scenario, future WLTP targets would be defined applying a correlation factor of 1,1 that does not envisage any credit for the shortcomings of the NEDC: 75-86 g/km for 2025 [7].

3 Powertrain Electrification

The CO_2 legislation framework presented in the preceding Sections implies a revision of the actual mobility solutions, aimed at moving towards technologies that limit the dependence from oil. In the long run, the objective is represented by a sustainable transportation, with vehicles propelled by energy coming from renewable sources or from hydrogen (FCEV *Fuel Cell Electric Vehicles*), but assuming that no major technological breakthrough is made over the next decades much of the total energy demand will continue to be satisfied by liquid fuels. The efficiency of internal combustion engine has already reached the limit, and the transition to a complete electrification of the vehicle (BEV *Battery Electric Vehicles*) is still an ongoing process: in these context Hybrid Electric Vehicles (HEV) assume a particular relevance. Combining two or more power sources on board, they are a sort of link between conventional and fully electric powertrains, and are considered one of the most promising and viable ways to lower the fuel consumption and meet the emission target in the near future. Despite not being the ultimate solution to the environmental issues, they allow to remedy some of the constraints typical of all-electric cars, such as reduced driving range, cause of the so-called range anxiety, high sticker price and the need for a dedicated charging infrastructure [11].

Giving a detailed description of all the various hybrid systems and their operating principles is out of scope for this thesis, however the following Section provides a brief overview for the sake of completeness.

3.1 Hybrid Architectures Overview

An Hybrid vehicle stores energy on board in two forms, combining the performance of a conventional internal combustion engine with an electric machine and a bidirectional electrical storage device. The fuel tank remains the primary energy source, but the increased flexibility in the energy conversion process allows to enhance the performance. A variety of HEVs is currently available on the market, and the classification is usually made with respect to the disposition of the various components or to the degree of hybridization. Considering the architecture, the possible solutions are *series*, *parallel*, and *series-parallel* or *complex* HEVs, while concerning the degree of hybridization the are *micro*, *mild* and *full performance* HEVs.

3.1.1 Series Hybrid

In a series hybrid vehicle, the ICE is not mechanically connected to the driving wheels and, being isolated from the power demand, can operate at its most efficient conditions activating the generator. The traction motor is generally powered by a battery pack, with the ICE/generator unit that helps or charges the batteries depending on the power demand rate. The mechanical transmission has usually a fixed transmission ratio, and considering the size of the hybrid module, it is possible to further classify series HEVs as [2]:

- *Range Extender:* it is a sort of thermally assisted electric vehicle, in which the ICE works at fixed operating point and it is used to charge the batteries. The engine is sized for the average power request over the driving cycle, and the overall range is related to fuel tank size (E.g. BMW i3 Range Extender);
- *Load Follower:* ICE and generator are designed to produce the maximum steady-state power. The engine follows the load time history during the cycle, switching between different operating points

on the Optimal Operating Line (OOL). During peak power transients, the power gap is provided by the battery pack;

- *Full Performance:* ICE and generator are designed to produce the maximum peak power. Performance is an aspect of primary importance, therefore the engine might be oversized to guarantee the possibility to drive the vehicle in case of failure of the electric module. This implies frequent ICE utilization at low-medium loads, where it is extremely inefficient;

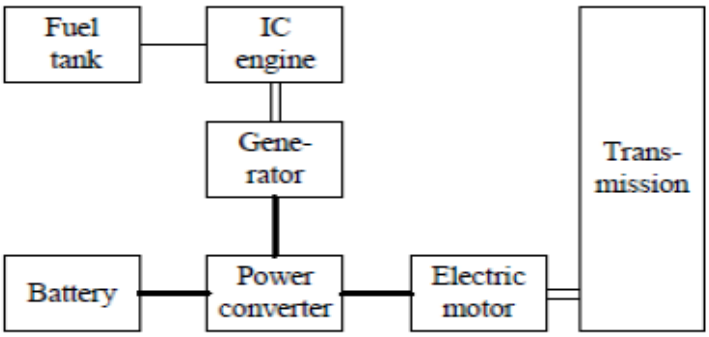

Figure 3.1: Series Hybrid powertrain schematization [12]

The need to convert the power output of the ICE into electricity to drive the electric motor and vice-versa leads to consistent inefficiencies (conversion factors lower than one), therefore series hybrid powertrains usually present a small ICE combined with a large battery back. This configuration has very low emissions and excellent efficiency during stop-and-go driving, because it minimizes inefficient engine operations and maximizes the energy recaptured from regenerative braking. At the same time, a heavy storage system negatively affects costs and performance, representing the major drawback of this configuration, and the ICE must be sufficiently powerful to meet minimum acceleration requirements in case of battery depletion.

3.1.2 Parallel Hybrid

In a parallel hybrid system, both the internal combustion engine and the electric motor can supply their mechanical power directly to the driven wheels. This solution allows to drive relying just on the batteries, just on the ICE or combining the two, eliminating the losses deriving from multiple energy conversions. As the maximum power of the system is approximately equal to the sum of the engine and electric machine figures, it can provide the same performance of a series hybrid but with downsized components. The control of a parallel hybrid drivetrain is on the other hand more complex, due to the mechanical coupling between the engine and the driven wheels and to the power-split management, and several configurations are available with respect to the linkage between ICE and EM.

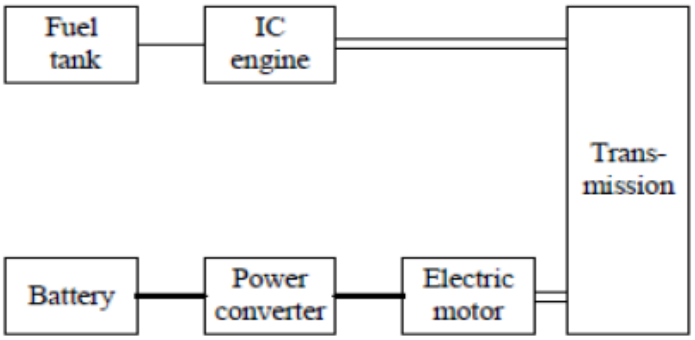

Figure 3.2: Parallel Hybrid powertrain schematization [12]

A further distinction between hybrid parallel layouts can be made depending on the positioning of the electric machine [2]:

- *P1f or P0* (or *Single shaft non coaxial*): the e-machine is connected to the engine at the front, considering a longitudinal layout (BAS or BSG);
- *P1r* (or *Single shaft coaxial without engine side second clutch*): the e-machine is on the crankshaft, between the engine and the clutch;
- *P2* (or *Single shaft coaxial with engine side second clutch*): the e-machine is situated within the engine and the transmission, with the capability to decouple it from the engine through a devoted clutch;

- *P3* (or *Double shaft*): the e-machine is downstream the transmission and differential unit, sometimes with a devoted ratio from e-machine shaft and secondary transmission shaft;
- *P4* (or *Double drive*): the e-machine is located on the secondary axle, typically linked to the differential through a devoted transmission;

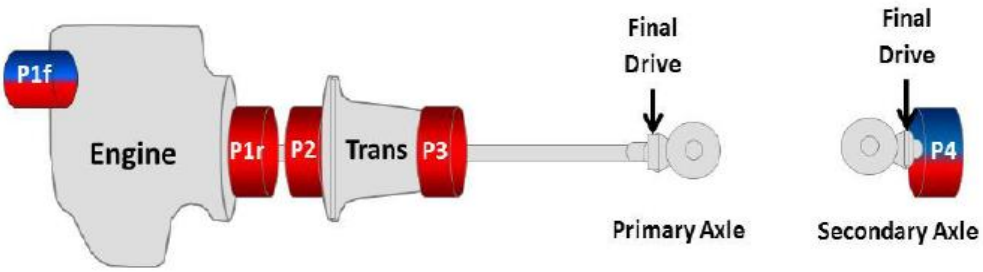

Figure 3.3: Parallel hybrids classification based on e-machine position [2]

3.1.3 Complex and Plug-in Hybrid

In literature, Complex Hybrids are also referred to as *Serie-Parallel* or *Combined Hybrids,* and mix the features of the above-mentioned solutions. Taking the 1997 Toyota Prius as an example, the presence of a double connection allows the power at the drive axle to be either mechanical, electrical, or both [13]. The power-split device or eCVT, incorporated in the powertrain, couples an ICE and two motor/generators (MG1 and MG2). It is a planetary gearbox with three input/outputs: the carrier, the ring gear and the sun gear which are connected respectively to ICE, MG1 and MG2. The system acts as a continuously variable transmission, able to vary the gear ratio between ICE and MG2 by controlling the speed of MG1, and removes the need for a traditional gearbox and transmission components. The smaller of the two motor/generators, MG1, is mainly used as a generator, whereas the larger MG2 operates as a traction motor and is directly connected to the wheels. The ICE rotation speed is limited between 1000 and 4500 rpm, and it does not directly affect vehicle speed [14].

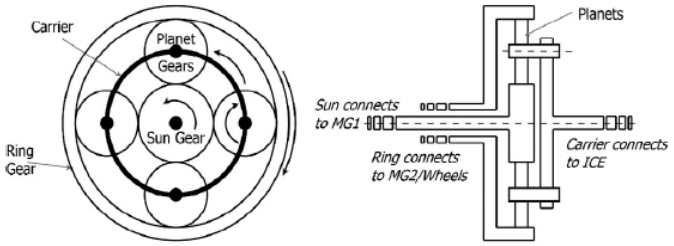

Figure 3.4: Complex Hybrid power-split device [14]

A Plug-in Hybrid (PHEV) has a rechargeable battery that can be restored by connecting it to an external electricity source, represented by a common socket a or a dedicated charging station. The vehicle is capable of running in pure electric mode as long as the battery depletes, and then works as a hybrid. Toyota has recently announced a plug-in version of the renowned Prius, with an increased battery capacity of 4.5 kWh and up to 11 miles of all-electric range. The retail prices on the Toyota website start at 33600€, conspicuously higher than the 24450€ request for the standard hybrid Prius mainly due to the enlarged battery size.

3.2 Focus on Low Voltage: Micro and Mild Hybrid

The identification of micro, mild and full performance parallel hybrids is based on a parameter named *Hybridization Factor* (HF):

$$HF = \frac{P_{EM}}{P_{EM} + P_{ICE}} = \frac{P_{EM}}{P_{TOT}} \tag{3.1}$$

where P_{EM} and P_{ICE} represent the nominal power of the electric motor and the internal combustion engine respectively. The HF is equal to zero for a conventional vehicle propelled by the ICE only, and equal to one for a battery electric vehicle. The values in between identify the different hybrid

configurations, with micro and mild hybrid placed in the lower part of the range.

Recently there has been a growing interest towards low voltage hybrids, since they are considerably cheaper than full hybrids and can provide up to 50 to 70% of the benefits with 30% of the costs. They can be divided into two categories, micro and mild hybrids, with on board electric power levels of about 3-5 kW and 7-12 kW respectively [13]. Moreover, on-board dc voltages below 60V do not require galvanic insulation for shock protection [15], and this contributes to limit complexity and costs.

3.2.1 Micro Hybrid

Micro-Hybrid is not considered a proper hybrid, as the power necessary to propel the vehicle comes uniquely from the internal combustion engine. The layout of the car remains the same, apart from the addition of a *Stop&Start* system, which turns off the engine when the car is stopped, e.g. waiting at a traffic light, and switches it back on as soon as the driver requests power. A small amount of regenerative braking might be achievable. This technology is based on a reinforced starter motor, able to handle the repeated cranking events, and no other modification of the powertrain is required. In recent years it has become a standard equipment on passenger cars, due to the positive impact on fuel consumption during city-driving, estimated in 8 to 15 % [14].

An example of a more advanced micro-hybrid system is the 2014 i-ELOOP developed by Mazda, based on an innovative supercapacitor that accept and delivers charge much faster than a conventional battery. The energy recovered during deceleration phases charges the supercapacitor (7-10 s), that in turn feeds the accessories for nearly a minute when the i-STOP (Stop&Start system) is active. During the fast-moving city driving, the supercapacitor repeatedly charges and discharges, being able to supply the

electric energy that would otherwise be collected from the battery/alternator.

As there are different schools of thought, the definition of micro-hybrid is not univocal, and some may include in this category the 12V Belt Starter Generator due to its restricted power figures.

3.2.2 Mild Parallel Hybrid

A Mild Parallel Hybrid is the identified as the basic level of powertrain electrification, and consists in replacing the engine starter motor and alternator with a single electric motor/generator unit that performs the tasks of both. With respect to a micro-hybrid, this configuration provides some extra torque to the ICE and extends the regenerative braking capabilities. The electric machine is named *Integrated Started Generator* (ISG), and generally provides no all-electric driving range due to the insufficient power output.

Various architectures have been designed, with different transmission systems and positioning of the electric machine: direct couple drive, chain drive, gear drive and belt drive. The following paragraph briefly describes each of these options [16], with the belt drive solution, object of this study, further analysed in Section 3.3.

- *Direct coupled drive:* in this layout, the motor generator unit is located on the engine crankshaft. There are two configurations available, one with the electric machine on the accessory side and one where it is placed in location of the flywheel. The amount of volume available allows to increase the size of the EM, and a large diameter machine might replace the flywheel rotor, guaranteeing a smooth torque delivery. However, to accommodate the starter/generator on the accessory side an extension of the shaft is required, thus creating a packaging issue in case the engine is mounted transversely;

- *Chain drive:* in this case the electric machine, that replaces the traditional starter, is placed directly into the transmission housing, which has to be redesigned. The coupling is realized by means of a chain that runs over a pulley, which causes relevant noise issues but represents a good compromise considering the lack of space. In fact, the major advantage of using a chain over a belt is the higher tensile strength, which allows a lower width and consequent packaging benefits.
- *Gear drive:* in this configuration the coupling of the electrical machine is realized on the transmission side (P2 or P3) by means of gears. The transmission housing needs to be modified, but the main drawback is represented by the gear teeth wear, that occurs at high speeds and low loads. The solution should be the use of elevated hardness materials or a multi-stage gear drive to lower the speeds, with a negative impact on costs.
- *Belt drive:* the coupling between the ICE and the electric machine is realized via a redesigned high-tension multirib belt, because of the higher load compared to a conventional vehicle. Being the electric motor placed on the accessory side, this configuration has a low impact on the original layout in terms of packaging, guarantees low noise levels and does not need any lubrication [17].

3.3 The Belt Starter Generator

The Belt Starter Generator, also denominated BSG or BAS, represents one of the most common architectures available for micro/mild parallel hybrid vehicles, where the traditional alternator is replaced by an electric motor-generator unit. The coupling with the electric machine is realized on the accessories side through a revised belt pulley tensioner, making this solution extremely easy to build and requiring a minimal amount of extra space if compared to a conventional powertrain. The electric machine can work either in motor or generator mode, providing additional torque for traction or storing energy during deceleration phases, but due to the structure of the system it is not possible to decouple the engine from the BSG and have the components working concurrently at optimum conditions. Another disadvantage of this layout is represented by the limited amount of power that can be transferred via a belt coupling.

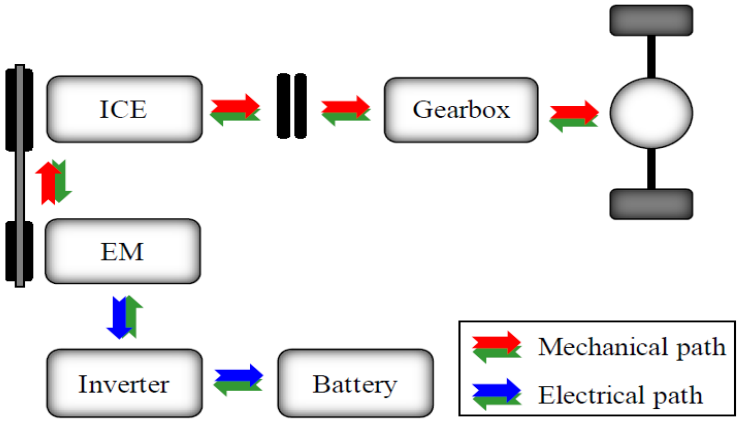

Figure 3.5: Powertrain layout of a BSG - equipped car [18]

The BAS solution is offered in two different configurations, 48V and 12V, with the latter usually regarded as a micro-hybrid, and Li-ion batteries are employed for the exploitation of the hybrid functionalities. The conventional 12V grid and lead acid battery are maintained to feed most of the on-board accessories, and for this reason in the most powerful setup the 48V battery is

linked to a DC/DC converter to lower voltage and current to suitable values. The inverter allows to change the direct current from the battery into alternating current for the EM.

3.3.1 Functions enabled

The functionalities of a Belt Starter Generator system can be gathered into two groups, primary and secondary, and this Section is aimed at describing their working principle and how they affect the vehicle drivability [16, 19].

Primary	*Secondary*
✓ Advanced Stop&Start	✓ Electrified auxiliaries
✓ Regenerative braking	✓ Engine coasting
✓ Torque assist	✓ e-Parking, e-AWD

Advanced Stop&Start

The major contribution to fuel saving in a BSG comes from the *Stop&Start* (S&S) system, that shuts down the ICE when it is not used to provide traction to the vehicle, thus eliminating engine drag torque at idling conditions. This strategy is particularly convenient when the vehicle is stuck in urban traffic and shifted into neutral, e.g waiting for a traffic light to turn green. As soon as the driver requests power, the cranking operation is performed quickly and smoothly by the motor-generator unit, without the noise from the starter motor gears. The “advanced” attribute refers to the extended range of action of the system: when coming to a stop, the engine is switched off while the vehicle is still on the move. However, a series of parameters must be monitored by the hybrid control system to decide whether to enable this strategy, and among these the most significant are the battery *State of Charge* (SOC) and the engine coolant temperature. The SOC is typically maintained between pre-defined limits to preserve battery life, and if it drops below a safety threshold the system is disabled and the ICE prevented from turning off. Regarding the engine coolant temperature, the S&S is activated after the

coolant has reached a temperature that guarantees optimum working conditions for the catalytic converter.

Regenerative Braking

The regenerative braking is a major functionality of a BSG system that operates during decelerations, when the energy required to rotate the electric machine, used as a generator, contributes to slow the car down. The kinetic energy of the vehicle, instead of being wasted as heat in the friction brakes, is partially recovered and stored in the battery, ready to be exploited to fulfil the needs of the electric loads or to be used whenever engine assist is needed. A greater stopping force means greater power generation, but for emergency stops or for substantial speed reductions the conventional disk brakes are employed. The BSG is in fact able to provide the entire brake power only for mild decelerations, and the mechanical brakes get into action as soon as the regenerative braking power limit is overcome. During these phases the engine continues to spin due to the mechanical linkage between ICE and MGU, the fuel injection is suspended and the pumping losses can be reduced in case the vehicle is equipped with a Variable Valve Timing (VVT).

This energy recovery mechanism requires on the other hand a modification of the conventional braking system, replaced by a *brake-by-wire* system in which the hydraulic connection between the pedal and the brake calipers is substituted by a specific actuator. The pedal position, as well as many other parameters, are then monitored by sensors to decide how to split the brake power.

Torque Assist

During accelerations, the energy stored during previous decelerations is used to drive the motor and consequently assist the engine. The electric machine dynamic behaviour allows for quick transients, and it is used to provide extra torque when the ICE is not capable of responding rapidly to the power demand. During vehicle starts or sudden acceleration requests by the

driver, the electric power assist might avoid a downshift and improves the vehicle drivability, providing the additional torque while the engine increases its speed. The transmission ratio of the BSG, which is an influencing parameter with respect to the torque available at the crankshaft, is typically in the range of 1:2 – 1:3 for a gasoline engine, depending on the characteristics of the motor – generator unit [17].

Secondary Functionalities

These BSG additional functions can be exploited to further improve the benefits in terms of fuel consumption and vehicle drivability. These features are usually a prerogative of the 48V layout, as the electric power demand would be too high for the least powerful configuration. It has to be mentioned that the 12V BSG, on top of the primary functions, allows also for some auxiliaries to be electrified, such as the air conditioning compressor, and for *Engine Coasting*. As soon as the driver releases the gas pedal with the gearbox engaged, the ICE back-driven by the transmission and a significant amount of energy is wasted due to frictions and pumping losses; during these phases, the ICE can be decoupled from the transmission by opening the clutch, and then set at idle speed (*Engine On Coasting*) or turned off (*Engine Off Coasting*). The reactivation of the engine can be performed by the BSG, but to enable this strategy on a manual transmission vehicle the presence of an *e-clutch* is required.

The BSG can also give an indirect contribution to fuel consumption reduction, as the extra torque provided by the motor generator unit might allow the use of downspeeding strategies. The loss in performance deriving from longer gear ratios would be balanced by the energy stored in the battery, enhancing the fuel efficiency.

3.4 State of the art and 48V systems

Recently, a growing number of manufacturers have started to offer micro and mild hybrid solutions, regarded as the simplest and cost effective solution to meet the objective of reducing pollutant gases emission in the near future. The state of the art is represented by the systems developed and supplied by Bosh, Continental, Delphi and Valeo, which are installed on a variety of different vehicles, from low-end A segment to luxury sedans. Currently in production, the 12V BSG Suzuki Swift 1.2, the 48V P0 Renault Scenic Hybrid Assist dci, the 48V P2 ISG Mercedes S Class 500. Audi has introduced a new mHEV family, based on the 12V BAS architecture for 4-cylinders engines and on the 48V for 6 an 8-cyclinders, with the Audi A8 that will benefit from the hybridization regardless of engine type.

Moreover, in October 2016 the European Union funded the *THOMSON* project, whose aim is to develop two different 48V architectures, integrating the e-machine either on the accessory side or between the engine and the transmission. Two different engine families were considered: a 1.6 litre diesel and a small downsized Spark Ignited CNG engine equipped with a direct injection system [20]. This testifies that low voltage hybrid architectures are believed to have the potential to quickly penetrate the market, enhancing the performance of the vehicle regardless the fuel type with lower emissions.

48V systems

The Ingolstadt car manufacturer itself is also known for being the pioneer in the introduction of a 48-volt electrical subsystem on a production car, the SQ7. The additional comfort and drivability functionalities offered in modern vehicles, along with the progressive replacement of the mechanical operated accessories with electric devices, have increased the electrical energy demand . As a consequence, the manufactures increased the voltage level, with the 48V identified as the best compromise for functionality, cost and

safety reasons. The 12-volt net will not be completely replaced any time soon, due to the power supply of traditional lighting and infotainment, but gradually all the components will be adapted or developed in a 48V perspective. Thanks to the higher voltage system, the Audi SQ7 is equipped with an electric turbocharger engineered by Valeo, which minimizes turbo-lag and enhances the CO_2 and fuel savings. An electromechanical system for the reduction of the body roll and the improvement of the ride quality is present as well, and uses an electric motor combined with a planetary gearbox. The SQ7 is just an example of how the increased voltage level promotes the electrification of several components, and the integration with a micro/mild hybrid powertrain would help to fully exploit their potential in terms of fuel consumption and CO_2 emission reduction.

4 Case Study

This Section provides an overview of the simulation activities of this thesis, describing the modelling approach and showing the targets and the achieved results.

4.1 Model Development

The literature review preceding this Section highlights the ongoing transition from conventional internal combustion engine vehicles to hybrid powertrains, pointing out low voltage technologies as the one of the most promising solutions to meet the future emission targets. The main purpose of the simulation is therefore to assess the benefits in terms of fuel consumption and CO_2 emission deriving from the adoption of a Belt Starter Generator. By means of the Matlab/Simulink software, the analysis was carried out on both the NEDC and WLTP cycles, which characteristics and peculiarities have already been discussed (Section 2.3).

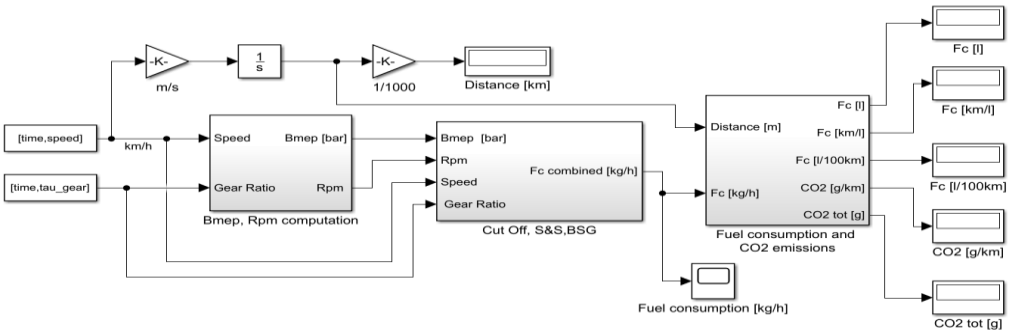

Figure 4.1: Simulink model

The vehicle chosen for the simulation was a gasoline A segment car, commonly referred to as *city cars*, and the three cases shown in Table 4.1 were studied:

	Fuel cut-off	Stop&Start	BSG
Case 1	✓	-	-
Case 2	✓	✓	-
Case 3	✓	-	✓

Table 4.1: Vehicle test cases

The *Stop&Start* entry refers to a conventional system, therefore it is not selected in Case 3 as the advanced version of this technology is integrated in the Belt Starter Generator.

Shown below are the main data relative to the modelled vehicle, and the different requirements of the two homologation cycles make it necessary to distinguish between three configurations. For this reason, some parameters are indicated side by side, respectively for *NEDC* and *WLTP low* or *high*. The two WLTP configurations corresponds to the minimum and maximum energy demand: considering the optional equipment available for the specific vehicle, "*low*" represents a base model whereas "*high*" represents a fully equipped one.

Vehicle			
	Segment	A	
	Unladen Mass	940	kg
	Test Mass	1020-1100-1180	kg
	Wheelbase	2300	mm
	Wheels Radius	291	mm
	F0	86.7 (116)	N
	F1	0.193 (0.065)	N/(km/h)
	F2	0.0317 (0.0358)	$N/(km/h)^2$

Table 4.2: Vehicle technical specifications

Engine		
Type	4 cyl in line, GDI	
Displacement	1242	cm^3
Maximum Power	51	kW @ 5500 rpm
Maximum Torque	102	Nm @ 3000 rpm
Idle Speed	800	rpm
Inertia	0.183	kg m^2
Fuel Density	720	kg/m^3
Fuel Lower Heating Value	44	MJ/kg
After-treatment System	EU 6	

Table 4.3: Engine technical specification

Transmission	
Gearbox Type	MT – 5 Speeds
Gear Ratio	1^{st} 3.91
	2^{nd} 2.174
	3^{rd} 1.48
	4^{th} 1.121
	5^{th} 0.897
Final Drive Ratio	3,438
Gear Ratio Efficiency	0.95
Final Drive Efficiency	1

Table 4.4: Transmission technical specifications

The *Case 3* test car is equipped with a 12V Belt Starter Generator, coupled by means of an inverter with a Li-ion battery and with a traditional lead acid battery. The latter is still present to feed most of the on-board accessories and performs the first cold cranking in combination with a traditional starter motor, thus originating a 12V + 12V architecture. The BSG carries out the following cranking operations once the Stop&Start logic is activated, and all the fuel saving functions are enabled thanks to the energy stored in the lithium battery. In the development of the Simulink model, some simplifications have been made: it was supposed that the engine fuel consumption map already included the mechanical accessories power

consumption, whereas an increase in the power demanded to the internal combustion engine was imposed to take into account the power absorption of the electric loads. Only the Li-ion battery has been modelled, and the lead acid battery maintained fully charged for the duration of the mission. The technical specifications of the electric machine and the Li – ion battery are reported in the following tables.

Electric Machine		
Type	BSG	
Maximum Power	Motor: 2,1	kW
	Regen: 8,8	kW
Maximum Torque	Motor: 13.7	Nm
	Regen: 21.4	Nm
Maximum Speed	20000	rpm
Weight	8,8	kg
Inertia	52*10^-4	kg m^2
Transmission Ratio	2	

Table 4.5: BSG technical specifications

Battery		
Type	Li-ion	
Capacity	11	Ah
Nominal Voltage	13,7	V
Configuration	4s1p	
Weight	4,3	kg
Operating Voltage	8 -16,8	V
Maximum Current	350	A
SOC Operating Range	0.9-0.4	

Table 4.6: Li-ion batery technical specifications

There are different approaches suitable for the development of vehicle mathematical models for the estimation of the fuel consumption and CO_2 emission, and the *Kinematic approach* was the one chosen for this research. It relies on the hypothesis that the homologation cycle is accomplished by an ideal driver, without any deviation from the imposed speed trace, and transient conditions are evaluated as a sequence of steady states. The

dynamic behavior of the system is neglected, and for this reason this methodology is traditionally used as a first step of the investigation. The power that the engine must provide is derived as a consequence of the vehicle speed through a so-called *backward* approach, considering the inertia force, the road loads and the driveline efficiency. Once the engine angular speed and load have been evaluated by means of kinematic relationships, the instantaneous fuel consumptions and pollutant emissions can be easily obtained from suitable 2D maps [21].

Concerning the gear shift strategy, it is imposed by the regulations regardless the vehicle type for the NEDC when a manual transmission is employed, whereas for the WLTP it was determined by means of a simple tool developed by Mr. Heinz Steven. The calculator accepts as input the vehicle technical data, along with parameters for modifying the execution of the cycle (Low or High configurations), and then gives back the gear shift profile as an output.

4.1.1 Fuel Consumption Computation

The evaluation of the fuel consumption starts from the vehicle main data, the drive cycle speed and gearshift profile and the efficiencies assumed for the various components of the powertrain. Part of the energy coming from the fuel burned throughout the mission is used to overcome the resistant forces and provide traction, while the rest is dissipated due to losses of various nature.

Knowing the speed profile of the mission and the gearshift profile, the engine speed can be computed using Eq 4.1 [21]:

$$\mathrm{n} = \frac{v[\frac{km}{h}] * 60 * \tau_{gear} * \tau_{final}}{2\pi * R[m] * 3{,}6}\ [rpm] \tag{4.1}$$

where R is the wheels rolling radius, τ_{gear} is the ratio of the selected gear and τ_{final} is the final drive ratio. If the resulting angular speed is below the idle

limit, the value of 800 rpm is imposed. The resisting force that opposes to the vehicle motion is computable in two different ways, using the aerodynamic drag and rolling resistances (4.2) or the Coast - down Coefficients (4.3):

$$F_{res} = F_R + F_{aero} + F_s = \mu_r mg + \frac{1}{2}\rho C_x A_f v^2 + mgsin\alpha \; [N] \quad (4.2)$$

where μ_r is rolling resistance coefficient, ρ the air density, C_x the aerodynamic drag coefficient and A_f the frontal section of the vehicle. The last term refers to the tangential component of the weight, and applies only when the longitudinal slope angle of the road is different from zero. The type approval tests provide that the vehicle is tested over a flat surface, therefore α is equal to zero. The second approach was chosen, employing coast-down coefficients obtained from tests conducted on the real vehicle.

$$F_{res} = F_0 + F_1 v + F_2 v^2 \; [N] \quad (4.3)$$

A fictitious equivalent mass has to be considered to take into account the inertia of the vehicle and of all the other components of the driveline that are rotating:

$$M_{app} = m_{vehicle} + J_{wheel}\frac{1}{R^2} + J_{ICE}\frac{{\tau_{gear}}^2{\tau_{final}}^2}{R^2} \; [kg] \quad (4.4)$$

where $m_{vehicle}$ represents the vehicle test mass, J_{ICE} and J_{wheel} the engine and wheels inertia respectively and τ_{gear} and τ_{final} the transmission ratio of the selected gear and the final drive ratio. The previous formula applies to a traditional internal combustion engine powertrain, and must be modified for modelling an hybrid car with an additional term that takes into account the presence of the electric motor generator unit.

$$M_{app} = m_{tot} + J_{wheels}\frac{1}{R^2} + J_{ICE}\frac{{\tau_{gear}}^2{\tau_{final}}^2}{R^2} + J_{em}\frac{{\tau_{gear}}^2{\tau_{final}}^2{\tau_{em}}^2}{R^2} \; [\text{kg}] \quad (4.5)$$

where m_{tot} is the overall mass and τ_{em} the transmission ratio of the BSG.

The power required at the wheels to follow the speed profile of the cycle can be computed multiplying the actual vehicle speed by the sum of the force necessary to overcome the road loads and the contribution of the inertia force during acceleration and deceleration phases:

$$P_{wheels} = \left(F_{res} + M_{app}\frac{dv}{dt}\right) * v \ [W] \tag{4.6}$$

By means of the transmission and final drive efficiencies it is possible to trace the engine power back.

$$P_{ICE} = P_{wheels} * \frac{1}{\eta_{transm} * \eta_{final\ drive}} \ [W] \tag{4.7}$$

The *Brake Mean Effective Pressure* (bmep) can finally be computed:

$$bmep\ [bar] = \ 1200 * \frac{P_{ICE}[kW]}{rpm * V[dm^3]} \tag{4.8}$$

Employing the *bmep* and the *rpm* as input data, a 2D lookup-table returns the instantaneous fuel consumption in kg/h, which is then integrated over the duration of the driving cycle to obtain the cumulative curves. The fuel consumption map also considers the portions of the mission where the vehicle is idling, e.g. when the required power and vehicle speed are equal to zero.

The CO_2 emissions are then determined by means of the following formula, employing the fuel density and the fuel consumption expressed in l/100 km:

$$CO_2[\frac{g}{km}] = \frac{\rho_{fuel}[\frac{kg}{dm^3}] * f_c[\frac{l}{100km}]}{0{,}0315} \tag{4.9}$$

4.1.2 Engine Warm-Up Model

A thermal sub-model was developed with the aim of estimating the trend of the engine coolant fluid temperature throughout the mission, which is the fundamental parameter to be monitored for the activation of the Stop&Start system. This Section provides a more detailed insight of the energy balance approach chosen.

Applying the first law of thermodynamics we obtain:

$$C_{H_2O}\frac{dT_{H_2O}}{dt} = W_{engine} - W_{heater} - W_{rejected} \tag{4.10}$$

where

T_{H2O}	coolant temperature	[°C]
W_{engine}	power to be dissipated	[W]
W_{heater}	power released by the cabin heater	[W]
$W_{rejected}$	power rejected from the radiator	[W]

$C_{H2O} = C_{cf} + C_{engine} + C_{oil}$

C_{cf}	thermal capacity of the coolant fluid	[kJ/°C]
C_{engine}	thermal capacity of the engine	[kJ/°C]
C_{oil}	thermal capacity of the lubricant	[kJ/°C]

The cabin heating system was supposed to be turned off, therefore the W_{heater} term equals to 0. The rejected heat is expressed by the equation here below:

$$W_{rejected} = h_{exc}(\dot{m_{CF}}, \dot{m_{AIR}})\left(T_{H_2O} - T_{outdoor}\right) \tag{4.11}$$

where h_{exc} [W/°C] represents the heat exchange coefficient of the radiator, which depends on the coolant fluid mass flow and on the air mass flow, and $T_{outdoor}$ is the temperature of the testing environment (23° C). The coolant fluid mass flow was imposed equal to 1 [kg/s], as it usually varies in a range

between 0,3 and 2 [kg/s]. The power to be dissipated was supposed equal to approximately a third of the energy released by the combustion process:

$$W_{engine} = 0{,}3 * \dot{m_b} * H_i \tag{4.12}$$

The front ventilator operating model was simulated taking into account the heat rejection requirements as well as the vehicle speed, with a formula that computes a virtual supplementary vehicle speed (Vent) that is added to the actual one in order to determine the air mass flow rate (4.14). Once the coolant fluid has reached the optimal working condition (90° C), the ventilator is activated and maintains a constant temperature.

$$Vent = 2\left[100\ P_1 - \frac{VS}{2}\right]\ \left[\frac{km}{h}\right] \tag{4.13}$$

$P_1 = T_{H2O} - 90$ if $T_{H2O} > 90$ [°C]

$P_1 = 0$ if $T_{H2O} = 90$ [°C]

VS = actual vehicle speed [km/h]

The air mass flow rate was computed as follows:

$$\dot{m_{AIR}} = c_f\ A_{fr}\ \rho_{AIR}\ v_{AIR} \tag{4.14}$$

with respectively

v_{air} = Vent + VS

c_f front end obstruction coefficient on air flow

A_{fr} radiator frontal area [m^2]

ρ_{air} air density [kg/m^3]

By applying the above-mentioned hypothesis:

$$C_{H_2O}\frac{dT_{H_2O}}{dt} = W_{engine} - h_{exc}\left(T_{H_2O} - T_{outdoor}\right) \tag{4.15}$$

$$\frac{dT_{H_2O}}{dt} + \frac{h_{exc}}{C_{H2_O}} T_{H_{2O}} - \frac{\left(W_{engine} + h_{exc} T_{outdoor}\right)}{C_{H_{2O}}} = 0 \qquad (4.16)$$

The resolution of the differential equation (4.16) allows to obtain the coolant temperature trend, which is showed in following Figure 4.1. The blue and red lines refer to the NEDC and WLTP cycles respectively, whereas the green line highlights how the Stop&Start system affects the warm up process on the NEDC. Compared to the baseline version, the optimal working temperature is in fact reached approximately 100 s later due to the amount of time spent with the engine turned off.

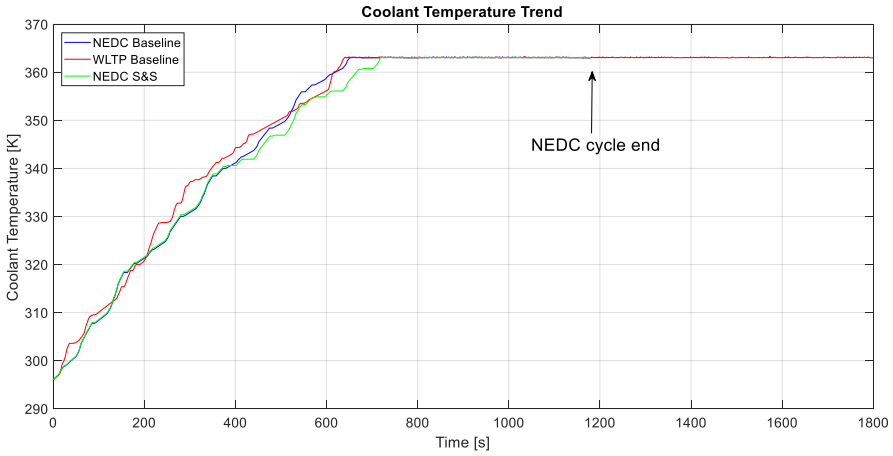

Figure 4.2: Coolant temperature trend

In order to simulate the cold start of the engine at the beginning of the homologation cycles, the fuel consumption values extracted from the 2D lookup-table have been divided by the factor showed in Figure 4.3, dependent on the coolant fluid temperature. These maps are in fact obtained with a warm engine, but during warm-up phases the frictions have a negative impact on engine efficiency, causing and increase of the consumed fuel As the coolant fluid temperature reaches its optimum working condition the factor progressively increases to one, meaning that the actual fuel consumption values correspond to the ones indicated in the map.

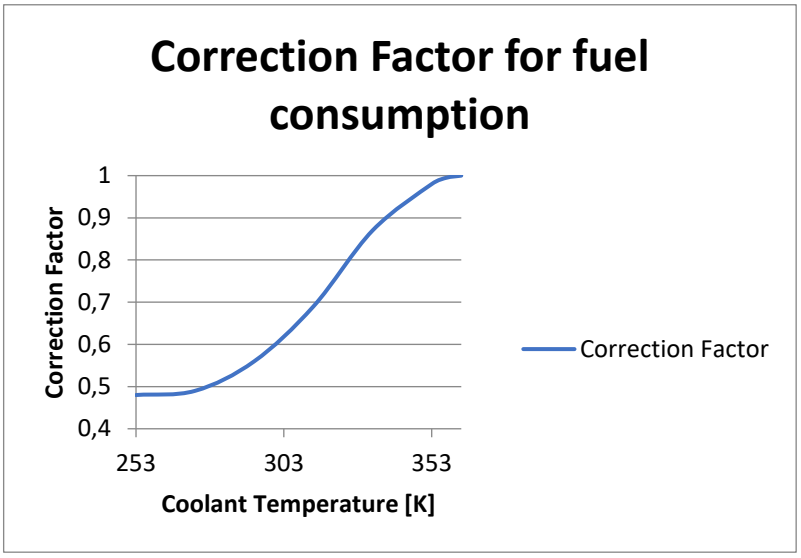

Figure 4.3: Correction Factor for fuel consumption

4.1.3 Battery Model

The motor-generator unit of the modelled vehicle is linked via a DC/AC converter to a Li-ion battery. This component was simulated using the equivalent resistance circuit down below:

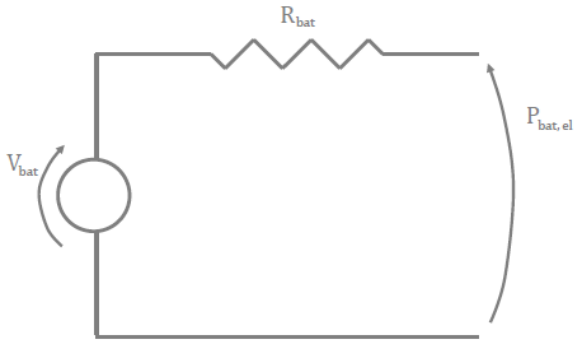

Figure 4.4: Li-ion battery equivalent circuit

The power balance of the system resulted in the following equation:

$$P_{batt,chem} = V_{batt} I_{batt} = P_{batt,el} + R_{batt} {I_{batt}}^2 \qquad (4.17)$$

where $P_{batt,chem}$ represents the power supplied by the battery, V_{batt} is the *open circuit voltage* (OCV), I_{bat} the battery current and R_{bat} the internal resistance.

Both OCV and internal resistance depend on the state of charge, and were determined using appropriate look-up tables. The battery current, derived from the following equation, was then employed to determine the *State of Charge* (SOC) variation in time.

$$I_{batt} = \frac{V_{batt} - \sqrt{{V_{batt}}^2 - 4R_{batt}P_{batt,el}}}{2R_{batt}} \; [A] \tag{4.18}$$

$$\frac{dSOC}{dt} = \frac{\int_0^t i \, dt}{Q} \tag{4.19}$$

The SOC represents a fundamental parameter to be monitored in a hybrid vehicle, as the activation of the fuel-saving functions of the BSG largely depends on its value. In a BSG application the battery is subjected to repeated charges and discharges that limit the life cycle, therefore the SOC operating range is usually limited to avoid ageing and improve the charge acceptance and efficiency during regenerative braking.

The motor generator unit is mechanically linked to the crankshaft by means of a belt-pulley transmission, and knowing the rotational speed of the ICE and the transmission ratio it is possible to trace back the electric machine angular speed:

$$n_{em} = n_{ICE} * \tau_{em} \tag{4.20}$$

The torque supplied by the BSG in motor and generation mode is indicated in the e-machine characteristic as a function of this parameter, and by means of the efficiency map the correspondent electrical power required to the battery can be determined.

4.1.4 Hybrid Strategy

Hybrid vehicles are equipped with an *Energy Management System* (EMS), which is responsible for the monitoring of several parameters with the aim of determining the optimal torque-split. Having two energy sources on board, the power flow is not directly controlled by the driver, as the EMS manages how to deliver the requested power. The control strategy in this case was designed to maximize the fuel consumption reduction, but other approaches could be used as well, e.g. oriented to obtain the maximum performance or to balance the various aspects according to the driving style.

For the application in question, a 12V Belt Starter Generator in position $P1_f$, the EMS assumes a marginal importance compared to a full-hybrid configuration, due to limited power output of the module both in motor and generator mode. The main purpose of the motor-generator unit is to extend the working range of a traditional Stop&Start system, combining it with regenerative braking and providing a little amount of torque assist at low rpms. The vehicle is propelled solely by the ICE, in the sense that all-electric driving is not possible in any condition. In this Section the implementation and the control strategy chosen for each of the BSG functionalities are discussed.

As previously mentioned, battery SOC is among the most important parameters to be checked by the hybrid controller for the activation of the BSG functionalities. Considering the selected battery operating range, the strategy considered three different cases:

- $SOC \leq SOC_{min}$: in case a previous discharge phase results in a low SOC, the engine would be prevented from switching off and the torque assist disabled, avoiding SOC to drop below the limit in a following cranking or assist event;
- $SOC_{min} < SOC < SOC_{max}$: as long as the state of charge remains between the limits, all the BSG fuel-saving functionalities previously described can be exploited;

〉 $SOC \geq SOC_{max}$: whenever the SOC reaches the upper limit, regenerative braking is inhibited and only the functionalities that discharge the battery are activated.

Advanced Stop&Start

The Stop&Start system was simulated by shutting off the engine whenever the vehicle is coming to a stop and shifted into neutral. If the speed decreases below the predefined threshold, the engine speed is reduced to zero and no fuel is consumed. The activation of the system is controlled by the coolant temperature, that must reach a minimum temperature of 35 °C. This threshold corresponds to the limit below which the catalytic converter cannot work properly, and emissions are remarkably high. If the value of the state of charge is too low, the available power from the battery might not be sufficient to crank the engine without dropping below the lower limit, and the strategy is therefore disabled. Once the system is active, to simulate the engine re-start after a stop phase a constant power absorption was imposed to the battery.

Advanced S&S ON when	• $SOC > SOC_{min}$ • Coolant temperature > 35 ° C • Speed < 15 km/h • Gearbox in neutral

Table 4.7: Advanced S&S activation strategy

Regenerative Braking

During the deceleration phases imposed by the speed profile of the cycle, two aspects contribute to the slowing down of the vehicle: coast-down components and proper braking. The necessary stopping force was computed as:

$$F_{decel} = m_v a = F - F_{road\ loads\ (-)} \tag{4.21}$$

where F is the force applied by the driver (negative in this case), $F_{road\ loads\ (-)}$ is the force opposed to the motion by rolling and air resistance and F_{decel} represents the inertia force deriving from the imposed deceleration a. Regenerative Braking is active only if $|F_{decel}| > F_{road\ loads\ (-)}$, when the driver has to operate the brake pedal as the required deceleration is greater than the share provided by the road loads only.

Powers were obtained multiplying the corresponding force by the speed, and to determine the maximum power recovered it was necessary to compare the instantaneous braking power required by the mission $P_{braking}$ with the amount of power that the BSG can actually regenerate, $P_{regen,max}$,

$$P_{braking} = (|P_{decel}| - P_{\ coastdown}) \tag{4.22}$$

In case the capabilities of the electric machine were sufficient for the regeneration of the entire braking power required, the phase was at the expense of the motor-generator unit and the energy recuperation was maximized; differently, the conventional friction brakes are enabled and the braking power is distributed between the two.

$$\begin{aligned} if\ P_{braking} \geq P_{regen,max} &\rightarrow P_{regen} = P_{regen,max} \\ if\ P_{braking} < P_{regen,max} &\rightarrow P_{regen} = P_{braking} \end{aligned} \tag{4.23}$$

It was checked whether the power available at the wheels for regeneration wss actually sufficient to overcome the frictions of the entire driveline and flow up to the Li-ion battery, otherwise no energy would be recovered.

The battery current during regenerative braking phases was limited according to the control law, as a function of the selected gear and the engine rotational speed, and the activation of the strategy was submitted to the SOC

value and to the engine rpm. The angular speed threshold has been chosen as consequence of the belt-drive transmission ratio and the mechanical characteristic of the BSG, to ensure that the electric machine worked in the maximum efficiency range.

Regenerative Braking ON when	• $SOC < SOC_{max}$ • Brake pedal pressed • Accelerator pedal released • In gear & gear ≠ 1 • Engine rpm > 1300

Table 4.8: Regenerative Braking activation strategy

The following figures show where the regenerative braking acted throughout the homologation cycles.

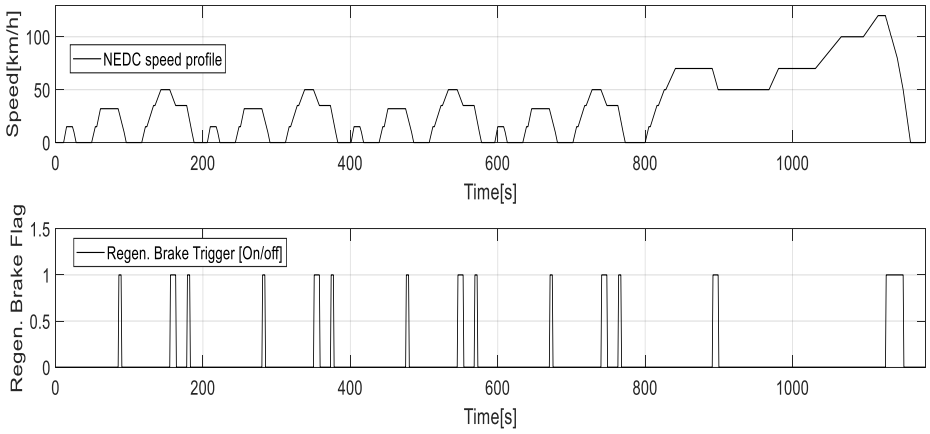

Figure 4.5: Regenerative braking activation flag, NEDC

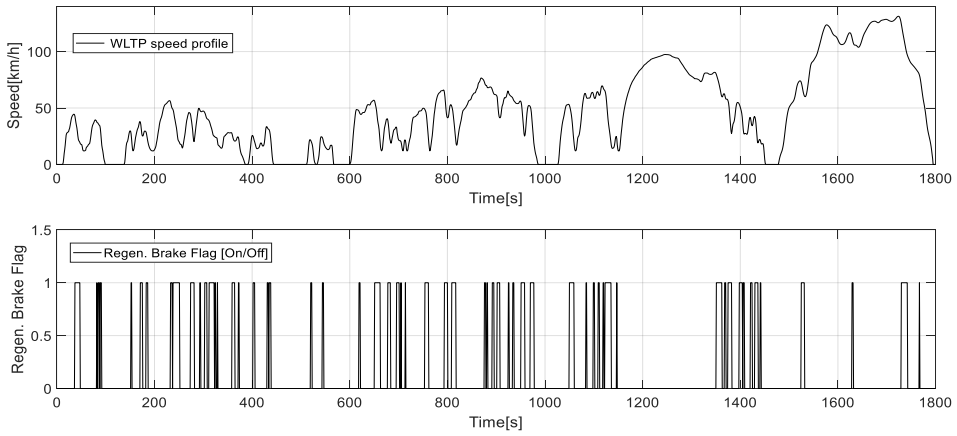

Figure 4.6: Regenerative braking activation flag, WLTP

On the NEDC almost every deceleration is good for energy recuperation, except for the first ramp of every ECE-15 cycle, where the deceleration happens in 1st gear at low speed and the regeneration does not activate. The WLTC speed profile, being more dynamic, offers the possibility of multiple regenerative braking events, usually of shorter duration compared to the NEDC.

Torque Assist

The restricted battery size represents the main constraint for the electric assist feature, and the motor-generator unit is employed mainly to enable a smoother acceleration following the engine restart. Provided that the SOC is sufficiently high, at low rpms the electric machine supplies the maximum power deliverable with respect to its angular speed; considering that the power demanded to the powertrain is imposed by the cycle, a portion of the request is fulfilled by the BSG, and this results in lower fuel consumption as the internal combustion engine load is reduced.

$$P_{ICE} = P_{required} - P_{em} \tag{4.24}$$

The transferable power, both in motor and generation mode, is further limited by the belt coupling, and for this reason an additional loss of 0,5 Nm that takes this aspect into consideration was envisaged.

Torque Assist ON when	
	• $SOC > SOC_{min}$ • Accelerator pedal pressed • Brake pedal released • In gear • Engine rpm < 2270

Table 4.9: Torque assist activation strategy

The logic was implemented to have the motor generator unit working in optimal conditions, and on the NEDC the torque assist gives its contribution predominantly after a stop phase, at the beginning of each ramp. The WLTC is more suitable to this BSG feature, especially for the low and medium sections representative of urban driving.

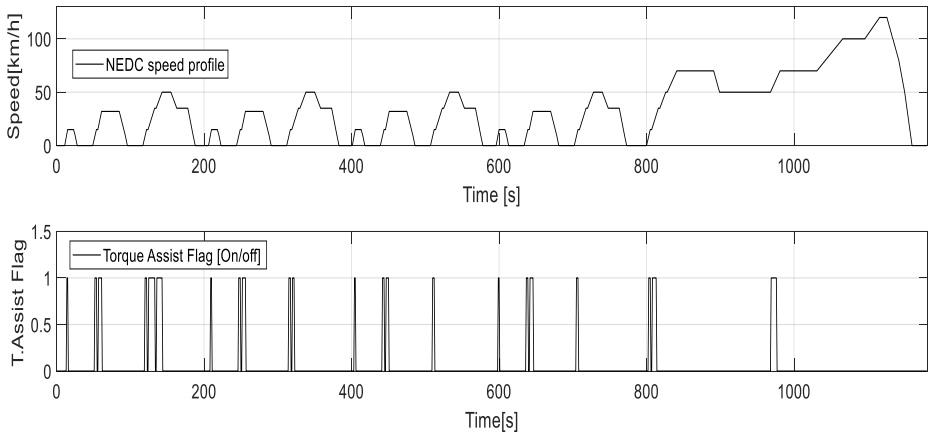

Figure 4.7: Torque assist activation flag, NEDC

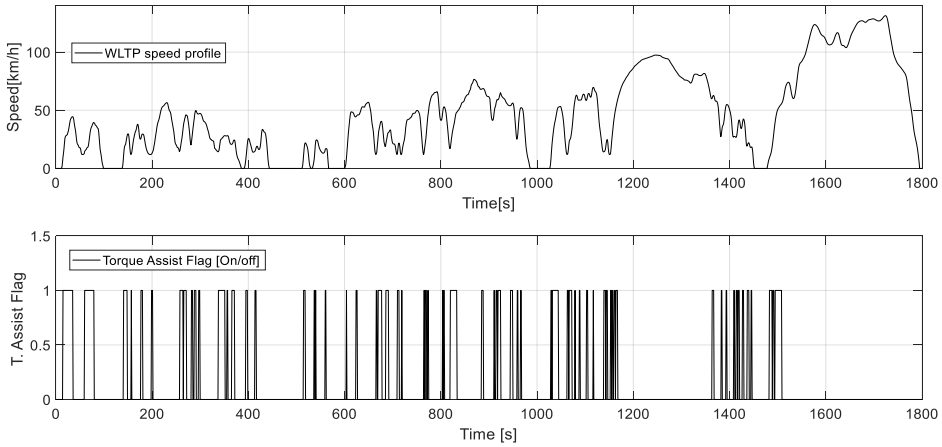

Figure 4.8: Torque assist activation flag, WLTP

4.2 Obtained Results

The application of the hypothesis and formulas discussed in the preceding Sections has allowed to quantify the benefits in terms of fuel economy and CO_2 emissions deriving from the use of a BSG architecture, which are here reported in the form of graphs and tables. The reference case is represented by a vehicle equipped with fuel cut-off only, in which the gasoline injection is interrupted whenever the driver releases the accelerator pedal and is reactivated when the engine speed reaches a certain threshold (200 rpm over the idle limit). A traditional Stop&Start system and a BSG have then been progressively added.

Depending on the driving cycle, the battery state of charge is subjected to different regulations. The *Case 3* vehicle belongs to the category of the traditional hybrid vehicles without an operating mode switch and not externally chargeable (NOVC), and it is classified as Class 3 with respect to the power-to-mass ratio for the WLTP. The NEDC procedure requires that for preconditioning two consecutive complete driving cycles are carried out without intermediate soaking. The vehicle shall then be kept in a room in

which the temperature remains relatively constant between the specified limits until the engine oil temperature and coolant are within +/- 2K of the temperature of the room. The third test is the one considered for the purpose of the homologation, and the results are corrected in function of the energy balance ΔE_{batt} of the vehicle battery, applying specific correction coefficients defined by the manufacturer. It is allowed to take the uncorrected values for fuel consumption and CO_2 emissions in case that ΔE_{batt} corresponds to a battery charging or to a battery discharging and ΔE_{batt} is within 1% of the energy content of the consumed fuel. The change in battery energy content can be calculated from the measured electricity balance al follows:

$$\Delta E_{batt} = \Delta SOC(\%) * E_{TEbatt} = 0{,}0036 * |\Delta Ah| * V_{batt} = 0{,}0036 * Q * V_{batt}\ (MJ) \qquad (4.25)$$

with E_{TEbatt} [MJ] the total energy storage capacity of the battery and V_{batt} [V] the nominal battery voltage [22].

The WLTP on the other hand requires this type of hybrid vehicle to be tested with one preconditioning cycle, followed by a cool down period. The emissions are determined with a test in *charge-sustaining mode* only, and consequently the SOC upper and lower limits were set at 65% and 45%. In order to avoid the correction, the initial state of charge of the Li-ion battery was imposed equal to final one for both NEDC and WLTP, and the preconditioning procedure started with a fully charged storage device.

Table 4.10 shows the results obtained from the simulations, and the cumulative fuel consumption curves are reported as well.

CO_2 Emissions [g/km]	**NEDC**	**WLTP Low**	**WLTP High**
Baseline	129	119	130
Stop&Start	122	116	126
BSG 12V	116	113	123

Table 4.10: CO2 emissions with cold start [g/km]

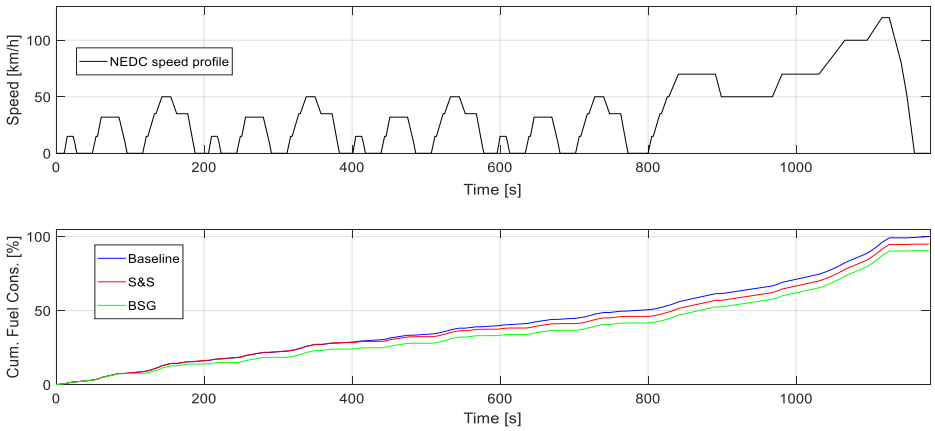

Figure 4.9: Cumulative fuel consumption on NEDC

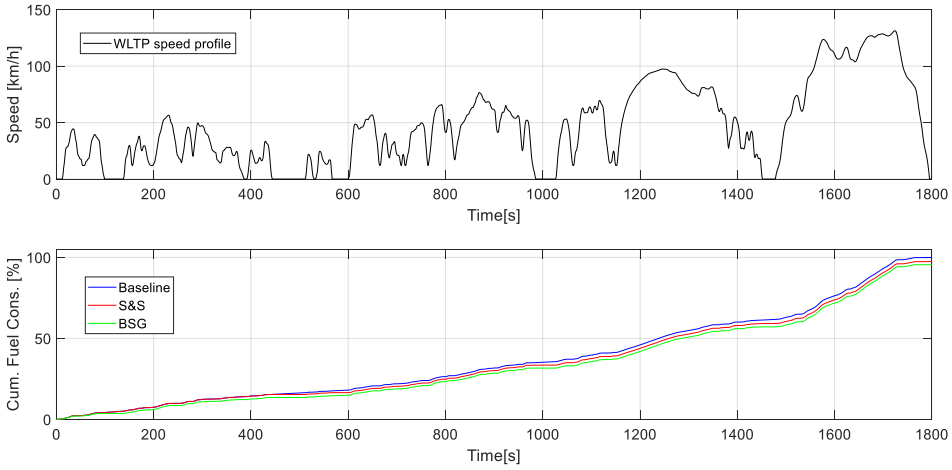

Figure 4.10: Cumulative fuel consumption on WLTP

Analyzing the data, it must be underlined how they reflect the differences between the two homologation cycles and the assumptions made for the realization of the model. For the baseline configuration, the WLPT emissions are lower or almost equal to the NEDC mainly for two reasons: the use of the same coast down coefficients for NEDC and WLTP Low and the correction factor applied for the simulation of the cold start. Comparing the results with simulations conducted starting with a warm engine (Table 4.11) it can be noticed that the WLTP High figures are higher than the NEDC, whereas the gap between WLTP Low and NEDC is reduced.

CO_2 Emissions [g/km] Warm Start	NEDC	WLTP Low	WLTP High
Baseline	119	115	125

Table 4.11: CO2 emissions with warm start [g/km]

The reason being is that the cold start has a lower impact on the new test procedure. The engine warm-up period has a similar duration for the two cycles, but being the WLTP considerably longer the correction factor influence on the emissions is approximately halved. The absolute values quoted above derive from the kinematic approach of the model, and therefore they might result to be different from the actual outcomes of the homologation procedures. This study, moving from the same initial conditions and hypothesis, is instead more focused on the benefits obtainable from the application of a low voltage technology.

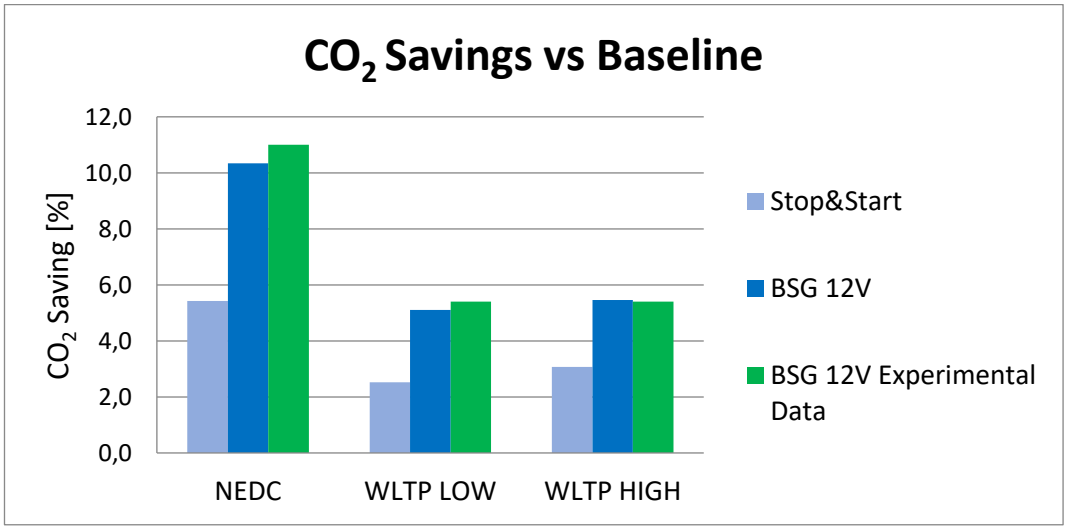

Figure 4.11: CO2 savings percentage with respect to the Baseline configuration

The CO_2 saving percentages in Figure 4.11 show that the application of a traditional Stop&Start technology is more beneficial to the NEDC compared to the WLTP, due to the higher stop share (23,7% vs 12,6%) . The BSG allows to extend the operating range of the S&S, as the engine can be turned off with the vehicle still moving, further increasing the gap. This aspect is the main

responsible for the difference between the two cycles in terms of overall benefit deriving from the belt starter generator. The histogram also displays the experimental data related to the application of the micro – hybrid technology on the real vehicle: the saving is comparable to the results obtained from the simulations, as a proof of the fact that the mathematical model, although simplified, is able to reproduce the actual impact of the technology.

The other major fuel saving function, the torque assist, has a better impact on the WLTP: the electric power assist events are in fact more frequent due to the increased dynamicity of the speed profile, and the BSG can contribute more substantially to the energy demand (Fig. 4.12).

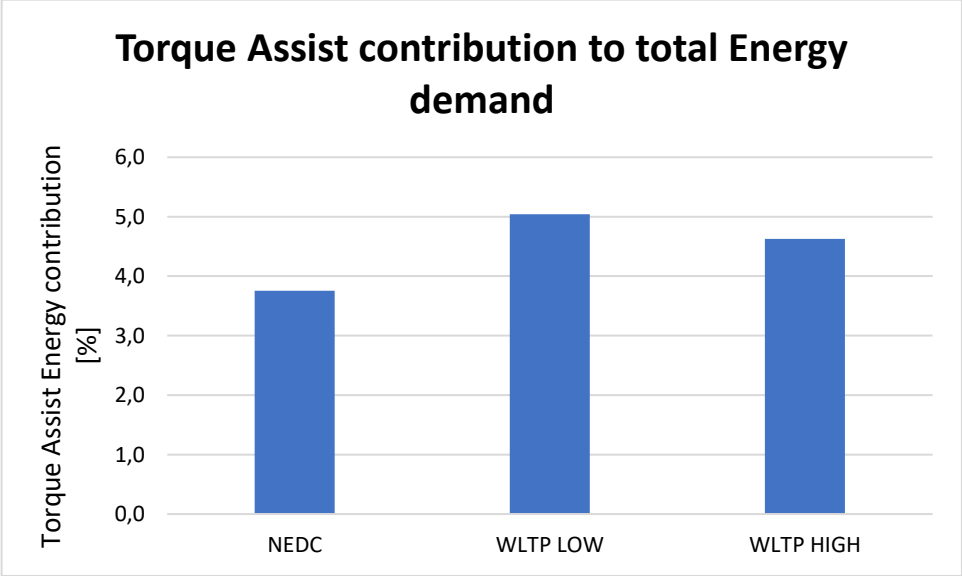

Figure 4.12: Torque assist contribution to total energy demand

However, even though the torque assist contribution to fuel consumption on the WLTP is higher, it is not sufficient to overcome the advantage related to the prolonged use of the S&S on the NEDC, and the final balance is favorable to the current homologation procedure.

The mathematical model has been validated also comparing the simulated engine speed profile to experimental data from a real vehicle equipped with a 12V BSG, and the result is depicted in the following figure:

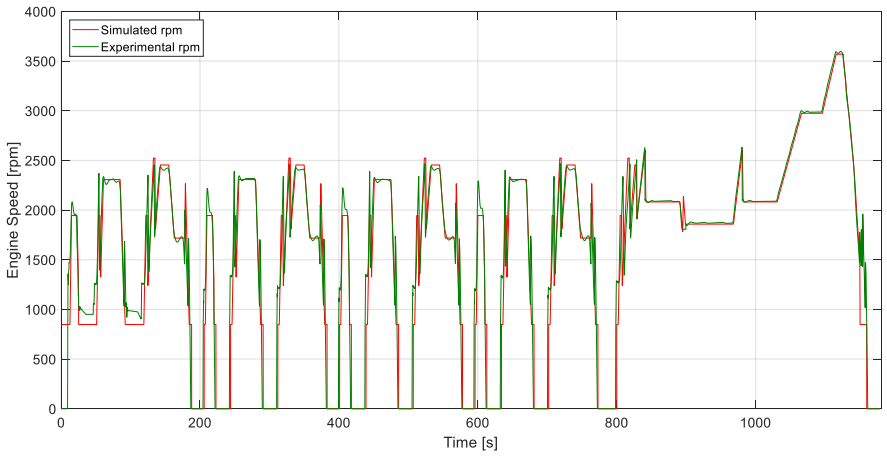

Figure 4.13: Simulated rpm vs Experimental rpm on NEDC

The engine stop phases have been simulated correctly, and the difference between the two profiles, attributable to the simplified kinematic approach adopted, has a negligible effect on the overall CO_2 emissions values.

4.3 E-clutch

As a further step of the investigation on low voltage technologies, the application of the E – clutch was simulated. This system represents an innovative solution for the hybridization of vehicles equipped with a manual transmission, thanks to which the driver can benefit from strategies such as engine coasting or electrically assisted driving, aimed at fuel saving. The mechanical link between the clutch pedal and the clutch itself is removed, and the system is governed by an electronic control unit which commands an electrical actuator. In case the acceleration is equal to zero and the vehicle is proceeding by inertia, the absence of pressure on the accelerator pedal is perceived by the sensors and the transmission is decoupled from the engine. The application of this technology on the modelled car is currently under study, in order to evaluate the contribution that its adoption would give over the homologation cycles.

To simulate the intervention of the e-clutch on the NEDC, some considerations and simplification have been made, starting from the analysis of the acceleration profile imposed by the mission. When the vehicle is decelerating, part of the braking power is provided by the aerodynamic and rolling resistances and part by the conventional friction brakes; if the deceleration required is lower than the share related to the coast - down components, the system could potentially be activated as the driver does not need to apply pressure to the brake pedal. The engine is then decoupled from the transmission, and set at idle speed (*engine-on* or *idle coasting*) or switched off (*engine-off coasting*) to reduce the fuel consumption. It has to be bear in mind that throughout the test the speed must remain within a tolerance band of +/- 2 km/h compared to the reference trace [10]; consequently, as soon as the velocity drops below the limit during coasting phases the gear must be engaged back or ICE has to be turned back on, operation that can easily be performed by the BSG.

The analysis on the NEDC revealed that the e-clutch system would never intervene throughout the mission, mainly for two reasons. The decelerations imposed by the speed profile are greater than those provided by the coast-down curve, requiring therefore the pressure of the brake pedal; during constant speed phases the activation of the coasting strategy should be theoretically feasible, but would rapidly cause a deviation of the velocity from the tolerance band. A modified NEDC profile has therefore been developed, with the aim of exploiting and estimating the potential of this eco innovation. Since every vehicle has a different coast-down curve, it is impossible to define a unique speed profile. The overall distance in the modified cycle and the distance covered at the end of the deceleration phases must be the same with respect to the original, meaning that once the coasting phase is terminated the profile to be followed is the standard one. Similarly, all the acceleration ramps and constant speed levels must be identical to the original NEDC. The engine coasting strategy is disabled if the speed is lower than 15 km/h, making the first ramp of each ECE-15 urban cycle useless at the scope, and can be activated two seconds after the vehicle has reached a steady speed. Moreover, the minimum time between the end of a coasting phase and the beginning of the following one is fixed at 4 seconds [23]. The modified cycle obtained is showed in Figure 4.14.

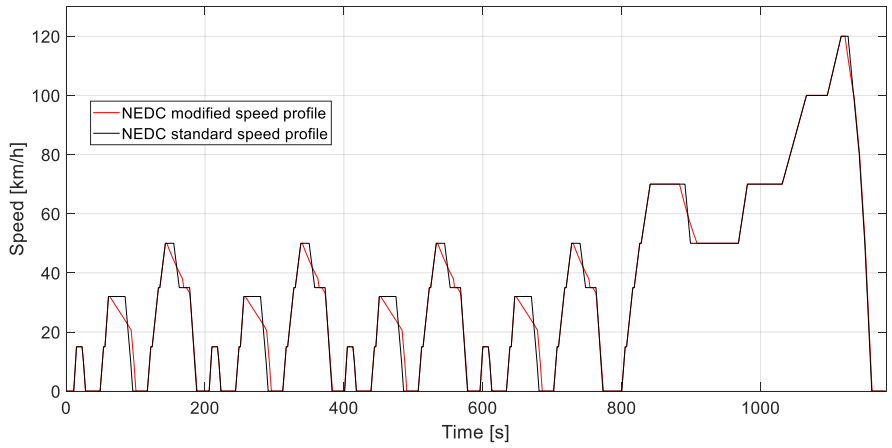

Figure 4.14: NEDC and modified NEDC speed profiles

The e-clutch system is enabled when the red line deviates from the black one, and deactivated when the two lines are parallel or overlap.

The baseline vehicle chosen for the analysis was equipped with fuel cut-off only (Case 1), and both the *Engine On coasting* and *Engine OFF coasting* configurations were simulated:

- Engine ON coasting: the gearshift profile has been modified (Fig. 4.15), selecting the neutral whenever a coasting event occur, and the ICE is set at idle speed with a consequent reduction in fuel consumption. The fuel cut-off logic is inhibited during the sailing phases;
- Engine OFF coasting: the ICE is turned off when the coasting strategy is activated, with the BSG responsible of the engine restart as soon as the driver presses any of the pedals. The torque assist and regenerative braking functions have been disabled for the purpose of this simulation, and the electric machine is employed uniquely for cranking operations. Due to coasting phases, the modified NEDC would imply a reduction in the amount of energy recoverable through regenerative, but the balance between the two strategies has not been investigated.

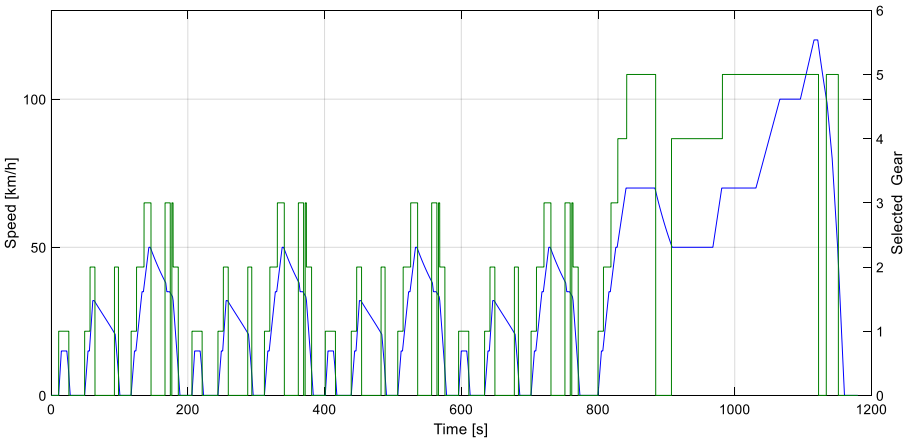

Figure 4.15: Modified gearshift profile for coasting

To consider the effective actuation time of the system, a time delay equal to 1 s was imposed in both cases, so effectively the coasting phases start 3 seconds after the beginning of the steady speed plateaus. The CO_2 emissions values obtained from the simulations are reported in the table below, along with the cumulative fuel consumption curves, but it has to be mentioned that the results overestimate the benefit obtainable from this eco-innovation. A specific procedure must in fact be followed by manufacturers.

	NEDC w/o Coast	**NEDC mod w/o Coast**	**NEDC mod Coast. En. ON**	**NEDC mod Coast. En. OFF**
CO_2 Emission [g/km]	129	125	120	112

Table 4.12: C02 emissions with Engine Coasting [g/km]

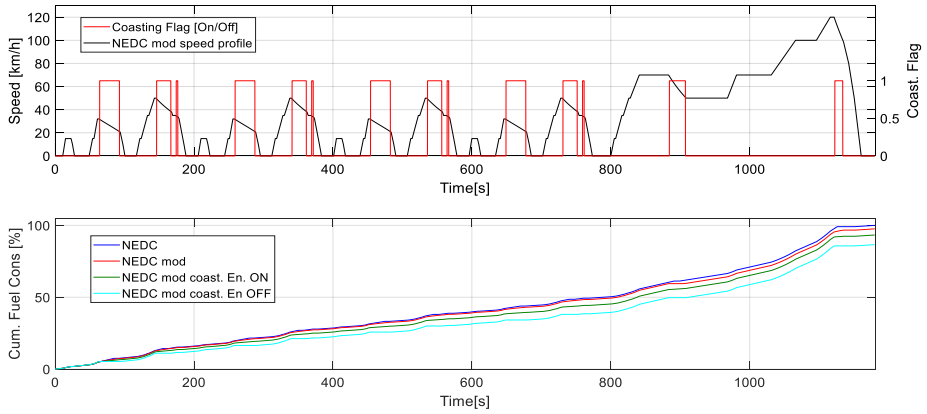

Figure 4.16: Cumulative fuel consumption on modified NEDC

To calculate the effective CO_2 savings for the purpose of the homologation the following equation should be used:

$$C_{CO_2} = \big((\text{BMC} - \text{EMC}) - (\text{BTA} - \text{ETA})\big) \cdot \text{UF} \tag{4.25}$$

with

C_{CO_2}: CO_2 savings [g/km]

BMC: CO_2 emissions of the baseline technology vehicle under modified testing conditions [g/km]

EMC: CO_2 emissions of the eco-innovation technology vehicle under modified testing conditions [g/km]

BTA: CO_2 emissions of the baseline technology vehicle under type approval testing conditions [g/km]

ETA: CO_2 emissions of the eco-innovation technology vehicle under type approval testing conditions [g/km]

UF: Usage factor (temporal share of technology usage in real world operation conditions)

The technology has been proven to give no benefit on the standard NEDC cycle, so the term (*BTA – ETA)* equals to zero. Regarding the usage factor UF, it is defined by equation (4.26)

$$\mathrm{UF} = \frac{\mathrm{RTC_{RW}}}{\mathrm{RTC_{mNEDC}}} \tag{4.26}$$

with

$\mathrm{RTC_{RW}}$: Relative time of coasting under real world conditions;

$\mathrm{RTC_{mNEDC}}$: Relative time of coasting under modified NEDC testing conditions.

Currently there are not sufficient data for an exact estimation of this correction factor for the tested vehicle, but other OEM have already carried out the homologation procedure of this technology as an eco-innovation. Considering the results obtained, a credible value of 0,6 has been selected for the UF. The CO_2 savings are then declared with respect to the baseline version tested under modified conditions, and are reported in the table here below and in Figure 4.17.

	NEDC mod w/o Coast	NEDC mod Coast. En. ON	NEDC mod Coast. En.OFF
Real CO_2 Saving [g/km]	-	-3	-8

Table 4.13: Engine Coasting CO2 savings vs BMC [g/km]

The effectiveness of the coasting strategy in real driving conditions is heavily influenced by the behaviour of the driver, and an aggressive drive style would not allow to exploit the full potential of this technology.

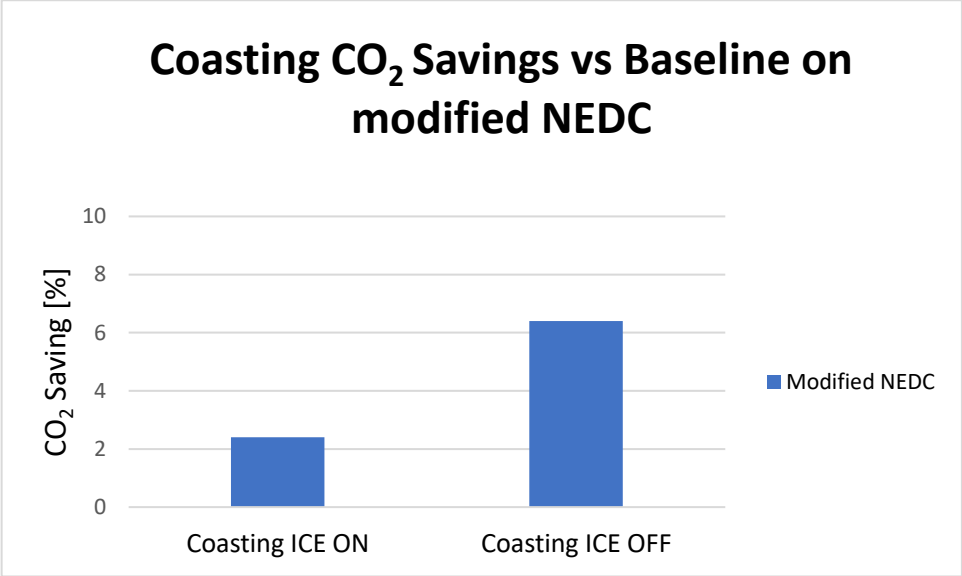

Figure 4.17: CO2 savings percentage with Engine Coasting vs BMC

4.4 Sensitivity Analysis

The purpose of the sensitivity analysis is to evaluate the impact on fuel consumption and CO_2 emissions caused by the change of some characteristics of the vehicle, both on the NEDC and WLTP. The components considered were the battery and the electric machine, and the results are discussed and shown below.

By changing the capacity of the Li-ion battery and the technical specifications of the motor generator unit, it might be possible to achieve a greater benefit from the fuel-saving functionalities introduced by the BSG, and several combinations have therefore been investigated with the aim of determining the optimal configuration in terms of cost per gram of $C0_2$ saved. The capacity of the storage device installed on the modelled hybrid car has been halved and doubled, though maintaining the same nominal voltage, coupling then each different battery to a 20% and 50% more powerful electric machine (Figure 4.18).

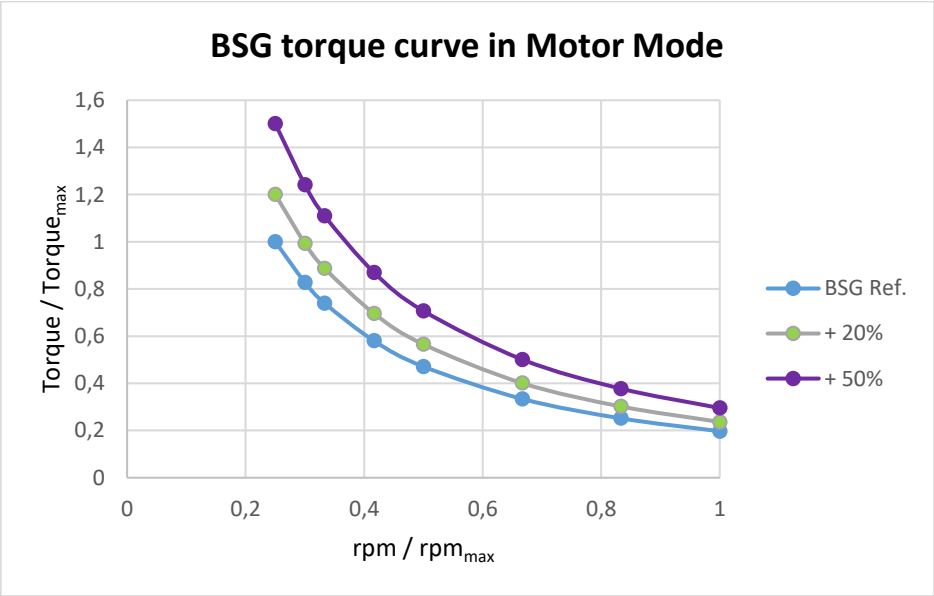

Figure 4.18: Different BSG torque curves, motor mode

The maximum acceptable current and the limits for the regenerative braking control law have been adapted to the increased power figures of the EM, in order to get the most out of the BSG.

Sensitivity Analysis

Battery	BSG
11Ah 12V (Reference)	2.1 $kW_{motor\ peak\ power}$ (Reference)
5 Ah 12V	+ 20%
20 Ah 12V	+50%

Table 4.14: Sensitivity analysis parameters

NEDC

The simulations revealed a negligible variation of emissions and consumed fuel over the homologation cycles, mainly attributable to the structure of the type approval procedure. The regulation imposes two preconditioning cycles for the NEDC, combined with the need to have the same SOC value at the beginning and end of the mission: these constraints affect the performance of this micro-hybrid powertrain. When starting the cycle valid for the purpose of the homologation, the battery energy content is usually modest, and the advantages that would derive from having larger and more capable components are almost cancelled. Considering the standard 11Ah battery, the first preconditioning cycle ends with a SOC of approximately 60%, which is the same level achieved after the second one, thanks to the energy recovered during the final brake from high speed (Fig. 4.19).

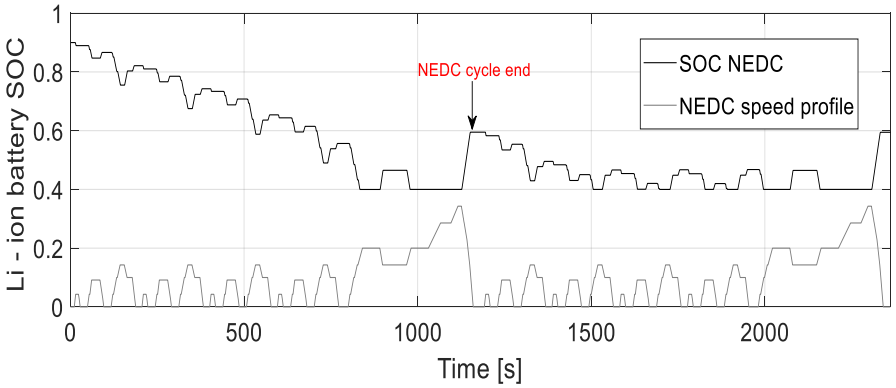

Figure 4.19: NEDC SOC trend during preconditioning

The SOC trend will remain the same for the following homologation cycle, and this aspect limits the use of the electric assist functionality as the battery reaches the minimum state of charge more frequently. The energy transferred thanks to the torque assist is almost 40% lower compared to a mission started with a fully charged storage device (Fig. 4.20)

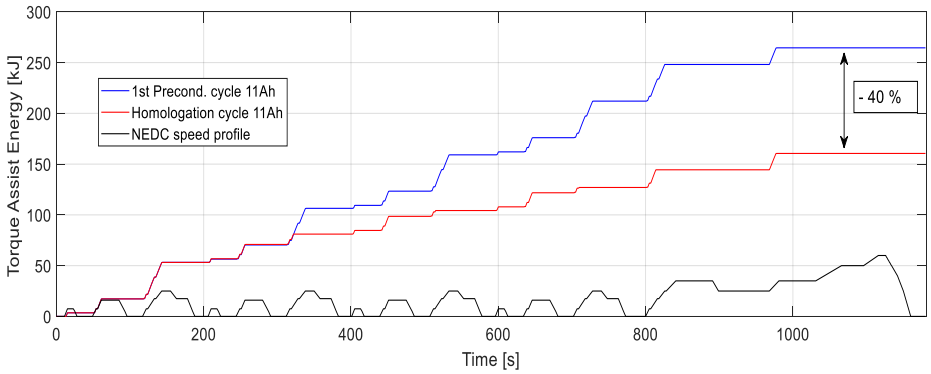

Figure 4.20: Torque assist energy after preconditioning, NEDC

Increasing the capacity of the battery, the negative impact of the preconditioning intensifies: the BSG expresses the maximum potential throughout the first cycle and the residual energy stored at the end of the procedure is even lower. On the other hand, a reduced capacity allows the battery to charge and discharge more rapidly (the electric machine is the same), with a minimum effect of the preconditioning on the CO_2 performance.

As a result, maintaining the hybrid control strategy and the BSG unchanged, the amount of energy supplied by the motor generator unit over the homologation cycle the is essentially the same with the different batteries (Fig. 4.21). The Stop&Start strategy has equal relevance for the three configurations, and being the torque assist the only other variable which affects the fuel consumption, the overall effect on the emissions is negligible.

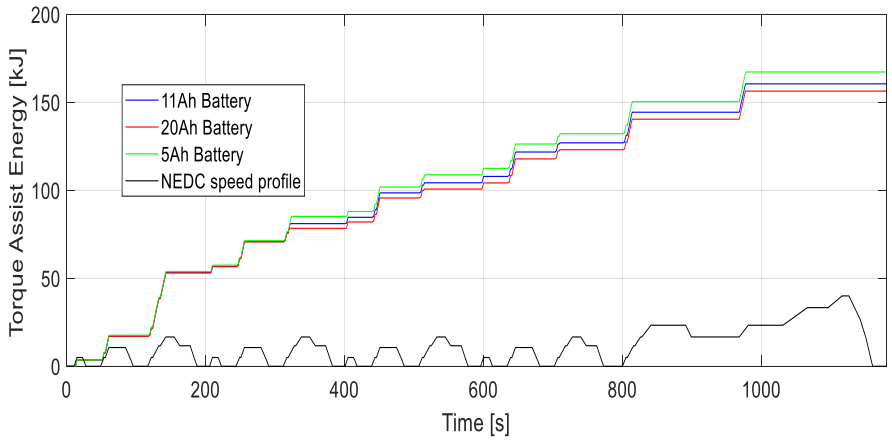

Figure 4.21: Torque assist energy with different batteries, NEDC

Upgrading the electric machine, the outcomes of the analysis are similar: the contribution of the BSG to the required torque, although increased, is not sufficient for a significant improvement of the CO_2 emissions, considering also the implications of to the preconditioning procedure beforehand discussed.

The only way to have a tangible benefit (1 g/km at least) from the different setups is running the simulations without considering the constraints of the testing procedure, starting with the Li-ion battery fully charged. The values obtained are useless for the purpose of the homologation, but are somehow more representative of real driving conditions, where the battery can exploit the entire state of charge range. Combining the 20Ah storage device with the 50% more powerful BSG the CO_2 saving compared to the reference case is quantifiable in 2 g/km, and even with the standard configuration an improvement of 1 g/km can be observed.

In conclusion, the emissions turned out to be barely influenced by the sizing of the components, but on the other hand it is not possible to neglect the impact on costs. Compared to the Stop&Start version, the following additional costs of the micro-hybrid system estimated by Ricardo have been considered:

System additional cost vs S&S

	BSG	BSG(Ref.)	BSG(+20%)	BSG(+50%)
Battery				
5Ah		250	300	350
11Ah (Ref.)		300	350	400
20 Ah		400	450	500

Table 4.15: Additional cost of the system compared to a S&S

The least expensive configuration, that matches the standard BSG with the 5Ah battery, is therefore the most convenient solution according to the simulations, in terms of € per g/CO_2 saved (Fig. 4.22). The choice of a larger storage device would probably guarantee more flexibility in a real application, but the simplified approach adopted does not allow to take this aspect into account.

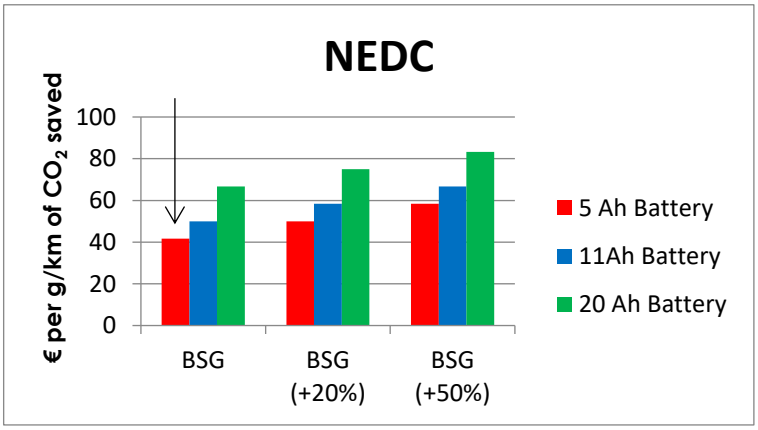

Figure 4.22: Optimal configuration, NEDC

WLTP

As required by the regulation for NOVC hybrid vehicles, the WLTP must be performed in charge sustaining mode after one preconditioning cycle. The feasible SOC operating range is therefore limited to 20% (65 to 45 %), and this constraint leads to slightly different results with respect to the NEDC. The test cycle is longer and more dynamic, therefore an increased capacity of the storage device allows to extend the use of the torque assist: the initial state of charge is imposed, and a larger battery will have a lower discharge rate provided the same power request. Figure 4.23 shows how the 5 Ah battery reaches the minimum SOC more rapidly compared to the other configurations, preventing the use of this functionality in the first part of the mission.

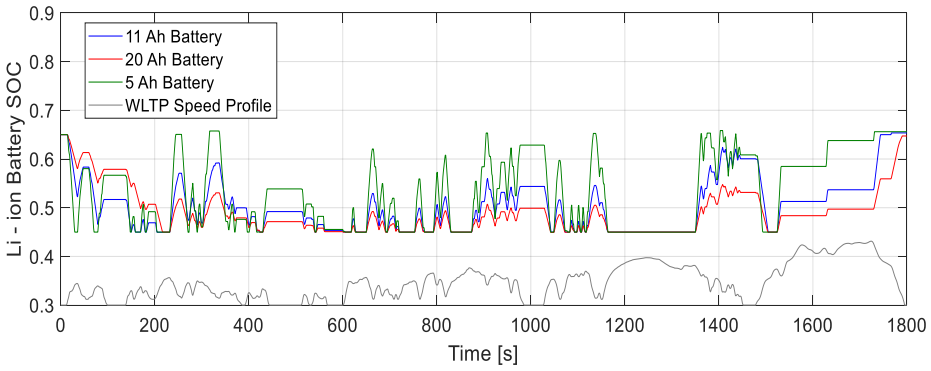

Figure 4.23: WLTP SOC trend with reference BSG

Increasing the power of the BSG, the two versions of the vehicle tested on the WLTP revealed a different behaviour: the *High* configuration is almost insensitive to the variations, with a maximum decrease of 1 g/km of CO_2 for the most powerful setup (with respect to the reference case), whereas for the *Low* configuration the reduction achieved is equal to 1 g/km with the 20% upgraded electric machine and 2 g/km with the 50% upgraded electric machine. The lower test - mass implies an inferior energy demand to cover the drive cycle, meaning that the overall contribution of the BSG is more substantial. For to the above – mentioned reasons, the 5Ah battery barley

allows an improvement in the CO_2 performance over the reference case, and between the 11Ah and 20Ah the differences are not significant (less than 1 g/km). The following tables report the benefits obtained for every configuration on the WLTP.

CO_2 Saving WLTP Low vs Reference case

Reference case: 113 [g/km]

	BSG (ref.)	BSG (+20%)	BSG (+50%)
5Ah Battery	(-)	(-)	-1 g/km
11Ah Battery (Ref.)	(-)	-1 g/km	**-2 g/km**
20 Ah Battery	-1 g/km	-1 g/km	**-2 g/km**

Table 4.16: CO2 saving vs Reference Case, WLTP Low

CO_2 Saving WLTP High vs Reference case

Reference case: 123 [g/km]

	BSG (Ref.)	BSG (+20%)	BSG (+50%)
5Ah Battery	+1 g/km	(-)	(-)
11Ah Battery (Ref.)	(-)	(-)	**-1 g/km**
20 Ah Battery	(-)	(-)	**-1 g/km**

Table 4.17: CO2 saving vs Reference Case, WLTP High

The analysis in terms of € per g/CO_2 saved has led to different results compared to the NEDC, so is not possible to define uniquely the most convenient combination of components. For the WLTP, the optimal configuration is represented by the 11Ah battery coupled with the most powerful electric machine, that guarantees an overall reduction of 5 g/km for the WLTP Low and 4 g/km for the WLTP High versus a traditional Stop&Start (Fig. 4.24, 4.25).

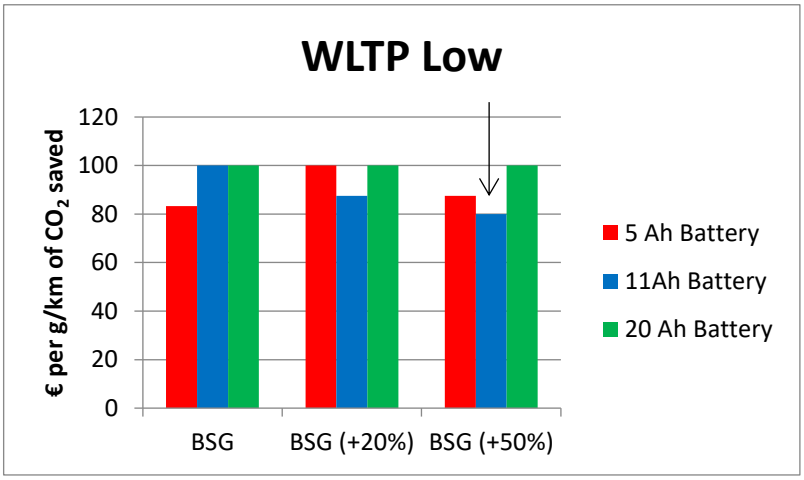

Figure 4.24: Optimal configuration, WLTP Low

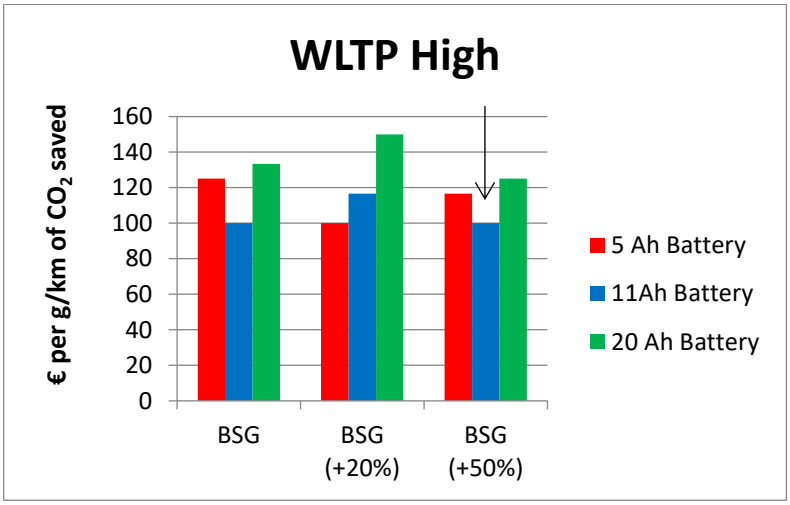

Figure 4.25: Optimal configuration, WLTP High

5 Cost – Benefit Analysis

It has been demonstrated that a low voltage hybrid solution has a positive impact on the environment, in terms of reduced fuel consumption and CO_2 emissions. However, to fully exploit their potential hybrid vehicles must be adopted on a large scale, and the penetration into the market is a consequence of their economic competitiveness. The purpose of the cost-benefit analysis is therefore to understand if both the automotive industry and the potential buyers are to benefit from this innovative technology. A greater initial investment is generally required to the customers to purchase a hybrid powertrain, and although the running costs are going to be lower due to the increased system efficiency it is fundamental to convince the clients that it is worth spending the extra money [14]. Clearly the benefits under real-world driving conditions are heavily influenced by the behaviour of the driver, so it is necessary to make some hypothesis for the evaluation of the real potential of this solution.

In a 2020 perspective, it was decided to conduct the study basing on the WLTP type approval procedure, considering the outcomes of the sensitivity analysis relative to the Low configuration, more representative of a city car.

The analysis started from the assumption that a potential buyer expects that the fuel saving would pay back the additional price of the BSG within 3 years. Considering the results of the simulations, along with an average gas price of 1,55 €/l, it is possible to calculate the fuel expense for a predefined annual mileage defined in accordance with the European statistics, and estimate the value that the customer would attribute to this technology. Within a few years every vehicle will be equipped with a traditional Stop&Start system, so it is more reasonable to measure the potential of the BSG with respect to this configuration.

Customer perspective

Annual Mileage: 15000 [km]
Time frame: 3 years

	Fuel Economy [l/100km]	**Fuel Price [€]**	**Annual Fuel Expense [€]**
Stop&Start	5,1	1,55	1185
BSG	4,9	1,55	1140

Table 5.1: BSG from Customer Perspective

The multiplication between the annual saving and the selected time frame gives back the maximum amount of money that a customer would be willing to pay for the technology:

$$3 * (1185 - 1140) \cong 135 \text{ €}$$

These results have to be examined from the manufacturer's perspective.

Considering the following hypothesis:

- Initial investment of 30 million € for the research and development activities;
- Useful life cycle of the technology of 5 years;
- Number of units produced per year: 100000. The depreciation costs for each unit equals therefore to 60 €.
- Additional cost for each unit vs Stop&Start: 400 €.

the overall production cost that the manufacturer has to support for the realization of a single BSG system is 460 €. The purchase price for the customer should be obviously higher, in order to guarantee a profit for the car company. Under this point of view the technology has no economic competitiveness, as the actual saving perceived by the customer is not sufficient to justify the greater initial expense.

However, the verdict on the feasibility of this micro-hybrid solution cannot be based only on the effective additional costs, but it is necessary to shift the focus to the regulatory framework. From 2019 on, the fine provided for not respecting the mandatory emission targets will be 95€ per gram of exceedance, and therefore for the producers the reduction of one g/km of CO_2 will be worth 95€. Being the BSG able to decrease the CO_2 emission values by 5 g/km compared to a conventional Stop&Start, the intrinsic value of the technology on the worldwide harmonized test procedure can be quantified in 475€.

Manufacturer perspective

Emissions premium	95 €/g
Saving vs Stop&Start	- 5 g/km
Additional Cost	460 €
BSG intrinsic value	475 €

Table 5.2: BSG from Manufacturer Perspective

In this context, the 12V BSG would represents an appealing solution for both the car makers and the final users: the amount of money saved avoiding the penalties exceeds the additional costs, and allows the manufacturer not to take a loss. To further increase the earnings, the producer could charge the clients an additional price over the traditional Stop&Start version: in this case the limit would be around 100 €, otherwise for an annual mileage of 15000 kilometres the technology would not pay back the investment within the prearranged period.

The ideal solution would be to offer the micro-hybrid configuration as a costless option, and exploit its potential with a suitable marketing strategy. From the customer perspective, it is clear that the improvement in fuel consumption envisaged, besides being largely dependent on the driving style, does not justify an extra charge, therefore it is not possible to define a retail price convenient for the manufacturer. Included as a standard equipment,

the BSG would on the other hand guarantee a return on the image of the brand, and lead potential buyers to appreciate and give credit to the technology. By means of an advertising campaign focused on the innovative fuel-saving functionalities introduced for free and on the implications of the homologation as a hybrid vehicle, the sales could be increased and the fixed costs reduced, making this solution gradually more convenient to the manufacturer. Moreover, it is essential not to overlook those aspects that are not directly monetizable, such as the benefits for the environment and humans' health deriving from the reduced emissions of air pollutants or the simple pleasure of owning and driving a hybrid. It is necessary to put a stress on the fact that micro/mild hybrids can be exempted from the payment of parking tickets and road tax, or are allowed access to limited traffic zones, rather than focus only on the mere advantages in terms of fuel consumption.

In the event that components costs undergo a reduction over the next years, the BSG will become more and more appealing for car makers, as a greater share of the additional costs could be charged to the customers maintaining the potential saving from penalties unchanged.

6 Conclusions

The European CO_2 regulation demands a 35% reduction of the fleet average emission target for passenger cars by the end of 2020, and more stringent requirements are expected for 2030. A revision of the current personal transportation model is needed, aimed at a progressive transition towards solutions that are less dependent on fossil fuels, and in this context hybrid powertrains represent the most viable solution to reduce the levels of air pollutants in the short term. This thesis was focused on low voltage electrification technologies, and particularly on the application of a 12V Belt Starter Generator on a gasoline A – segment car. The potential of this technology in terms of fuel consumption and CO_2 emissions reduction has been evaluated by means of a simple mathematical model, on both the NEDC and WLTP test cycles, and validated by means of experimental data. A baseline and Stop&Start configurations have been modelled as well for the estimation of the relative savings. The simulations showed that this solution is more beneficial on the NEDC (-6 g/km vs S&S), mainly because the peculiarities of the speed profile are more suitable to the characteristics of this micro hybrid system, guaranteeing a prolonged use of the most effective fuel – saving functionality provided by the BSG, the advanced Stop&Start. On the other hand, the longer duration of the WLTP, combined with a limited use of the S&S and with the constraint of the charge sustaining mode, resulted in a lower contribution of the BSG to the total energy demand and a consequent lower impact on the CO_2 emissions (-3 g/km vs S&S).

As a further step of the investigation on low voltage technologies, the effect of the installation of an e-clutch has also been evaluated: this technology enables engine coasting strategies with a manual gearbox, decoupling the engine from the transmission in case the driver releases the pedals and the vehicle is proceeding by inertia. Considering the coast – down coefficients of the tested car a suitable modified NEDC profile was realized, and the

evaluation the actual benefit deriving from the use of this eco - innovation was carried out according to the regulation. Compared to a baseline configuration, the reduction of CO_2 emissions was remarkable (≈ 2% with engine-on coasting and 6% with engine-off coasting), and further improvements could be obtained with the combination of e-clutch and BSG, especially in urban driving conditions. It has to be mentioned that the effectiveness of this system in a real-world application is strongly affected by the driving style, and the user must be aware of the working principle of the technology and inclined to fully exploit its potential.

The sensitivity analysis, performed with respect to the capacity of the Li – ion battery and the power figures of the Belt Starter Generator, has underlined the impact of the preconditioning procedure that precedes the cycle valid for the purpose of the homologation. For the NEDC, the result was a negligible variation (< 1g/km) of the CO_2 emission values between the various configurations considered, and this allowed to select the lowest cost option as it guarantees the same saving with a lower expense. The WLTP showed a different sensitivity to component sizing, and a limited improvement in the CO_2 performance compared to the reference case was achieved employing a slightly more powerful electric machine. The *Low* configuration benefited more from the upgrade of the micro hybrid system (-2 g/km vs Ref.), as a consequence of the reduced test mass and energy demand, and turned out to be the most convenient solution in terms of € per gram of CO_2 saved.

The cost – benefit analysis revealed that the 12V BSG is an option that could be taken into consideration by manufacturers, as the potential penalties avoided thanks to the reduced emissions would overcome the additional cost of the technology. The mere advantages in terms of fuel consumption for the customer would not justify a substantial additional expense compared to a S&S, but highlighting the advantages of the homologation as a hybrid a greater share of the costs could be charged to the client. The sales would be enhanced as well, with a consequent beneficial effect for the environment.

Bibliografy

[1] European Automobile Manufacturer Association. *http:// www.acea.be/statistics/article/world-passenger-car-production.* December, 2017.

[2] Ezio Spessa. "Controllo delle emissioni inquinanti" lecture notes. Politecnico di Torino, 2016.

[3] International Energy Agency. *CO_2 Emissions from Fuel Combustion: Overview, 2017.*

[4] StudentEnergy. *https://www.studentenergy.org/topics/conventional-oil.* December 2017

[5] Inernational Energy Agency. *2008 World Energy Outlook.* Pp 252-253, 2008.

[6] International Council on Clean Transportation. *EU CO_2 emission standards for passenger cars and light-commercial vehicles.* ICCT, 2014.

[7] Peter Mock. *2020-2030 CO_2 standards for new cars and light commercial vehicle in the European Union.* ICCT, 2017.

[8] Georgios Fontaras, Nikiforos-Georgios Zacharof, Biagio Ciuffo,. *Fuel Consumption and CO_2 emissions from passenger cars in Europe – Laboratory versus real-world emissions.* Elsevier, Progress in Energy and Combustion Science, 2016.

[9] Peter Mock, Jorg Kuhlwein, Uwe Tiegte, Vicente Franco, Anup Bandivadekar, John German. *The WLTP: How a new test procedure will affect fuel consumption values in the EU.* ICCT, 2014.

[10] E/ECE/324, Regulation 101 of the European Commission. *Concerning the adoption of uniform technical prescriptions for wheeled vehicles, equipment and parts which can be fitted and/or be used on wheeled*

vehicles and the conditions for reciprocal recognition of approvals granted on the basis of these prescriptions. European Commission, 2005.

[11] Alessandro Ferrari, Edoardo Morra, Ezio Spessa. *Analysis of Energy Efficient Management of a Light-Duty Parallel-Hybrid Diesel Powertrain with Belt Starter Generator*. SAE International, 2011

[12] Aldo Boglietti, Silvio Vaschetto. "Trazione Elettrica" lecture notes. Politecnico di Torino, 2017

[13] Behzad Asaei, Mohammed Kebriaei, Abolfafz Halvaei Niasar. *Hybrid Electric Vehicles: An Overview.* International Conference on Connnected Vehicled and Expo (ICCVE), 2015.

[14] Tim Hutchinson, Stuart Burgess, Guido Herrmann. *Current hybrid-electric powertrain architectures: Applying empirical design data to life cycle assessment and whole-life cost analysis.* Elsevier, Applied Energy, 2013.

[15] R. Bojoi, S. Rubino, A. Tenconi, S. Vaschetto. *Multiphase electrical machines and drives: A viable solution for energy generation and transportation electrification.* International Conference and Exposition on electrical and Power Engineering, pp.632-369, 2016.

[16] Stefano Baldizzone. *Performance and Fuel Economy Analysis of a Mild Hybrid Vehicle equipped with a Belt Starter Generator.* University of Windsor, 2012.

[17] Shaotang Chen, Bruno Lequesne, Rassem R. Henry, Jeffrey J. Ronning, Yanhong Xue. *Design and testing of a Belt-Driven Induction Starter-Generator.* IEE Transaction on Industry Applications, Vol 38, pp 1525-1533, 2002.

[18] Edoardo Pietro Morra, Ezio Spessa, Mattia Venditti. *Optimization of the operating strategy of a BAS Hybrid Diesel Powertrain on Type-Approval*

and Real-World representative driving cycles. ASME International Combustion Engine Division Spring Technical Conference, 2012.

[19] Marco Cossale. *Multi-phase Starter–Generator for 48V Mild–Hybrid Powertrains.* Politecnico di Torino, 2017.

[20] European Commission, CORDIS, Thomson Project. *https://cordis.europa.eu/project/rcn/205673_en.html.*

[21] Federico Millo. "Propulsori Termici" lecture notes. Politecnico di Torino, 2016

[22] EUR – Lex 42007X0619(02). *Regulation No. 101 of the Economic Commission for Europe of the United Nations (UN/ECE)*, *addendum 100.* European Commission, 2007.

[23] EU Implementing Decision 2015/1132. *On the approval of the Porsche AG coasting function as an innovative technology for reducing CO_2 emissions from passenger cars pursuant to Regulation (EC) No. 443/2009 of the European Parliament and of the Council.* European Commission, 2015.